Nonlocality and intermittency in three-dimensional turbulence

J-P. LavalB. DubrulleS. Nazarenko

Nonlocality and intermittency in three-dimensional turbulence

J-P. Laval
Institute of Geophysics and Planetary Physics, University of California Los Angeles, 3845 Slichter Hall, Los Angeles, California 90095

B. Dubrulle
*CE Saclay, F-91190 Gif sur Yvette Cedex, France
and CNRS, UMR 5572, Observatoire Midi-Pyrénées, 14 Avenue Belin, F-31400 Toulouse, France*

S. Nazarenko
Mathematics Institute, University of Warwick, Coventry CV4 7AL, United Kingdom

Numerical simulations are used to determine the influence of the nonlocal and local interactions on the intermittency corrections in the scaling properties of three-dimensional turbulence. We show that neglect of local interactions leads to an enhanced small-scale energy spectrum and to a significantly larger number of very intense vortices (''tornadoes'') and stronger intermittency (e.g., wider tails in the probability distribution functions of velocity increments and greater anomalous corrections). On the other hand, neglect of the nonlocal interactions results in even stronger small-scale spectrum but significantly weaker intermittency. Thus, the amount of intermittency is not determined just by the mean intensity of the small scales, but it is nontrivially shaped by the nature of the scale interactions. Namely, the role of the nonlocal interactions is to generate intense vortices responsible for intermittency and the role of the local interactions is to dissipate them. Based on these observations, a new model of turbulence is proposed, in which nonlocal (rapid distortion theory-like) interactions couple large and small scale via a multiplicative process with additive noise and a turbulent viscosity models the local interactions. This model is used to derive a simple version of the Langevin equations for small-scale velocity increments. A Gaussian approximation for the large scale fields yields the Fokker–Planck equation for the probability distribution function of the velocity increments. Steady state solutions of this equation allows one to qualitatively explain the anomalous corrections and the skewness generation along scale. A crucial role is played by the correlation between the additive and the multiplicative (large-scale) process, featuring the correlation between the stretching and the vorticity. © *2001 American Institute of Physics.* [DOI: 10.1063/1.1373686]

I. INTRODUCTION

A puzzling feature of three-dimensional turbulence is the large deviations from Gaussianity observed as one probes smaller and smaller scales. These deviations are usually believed to be associated with the spatial intermittency of small-scale structures, organized into very thin and elongated intense vortices (''tornadoes'').[1–3] They are responsible for anomalous corrections to the normal scaling behavior of structure functions associated with the Kolmogorov 1941[4] (K41) picture of turbulence. In this picture, energy-containing structures (the so-called ''eddies'') at a given scale interact with other eddies of smaller but comparable size to transfer energy at a constant rate down to the dissipative scale. A simple prediction of this local picture of turbulence is the famous $k^{-5/3}$ energy spectrum, which has been observed in numerous high Reynolds number experimental data and numerical simulations. The local theory of turbulence further leads to the prediction that the nth moment of a velocity increment $\delta u_\ell = u(x+\ell) - u(x)$ over a distance ℓ should scale like $\ell^{n/3}$. This behavior has never been observed in turbulent flows, and it is now widely admitted that anomalous corrections exist at any finite Reynolds number.

Various scenarios have so far been proposed to explain and compute the anomalous corrections. To mention but a few: spatial intermittency of the energy dissipation,[5] multifractal scaling,[6] large deviations of multiplicative cascades,[7] extremum principle,[8] zero modes of differential operators,[9] scale covariance. These approaches all try to model the breakdown of the exact local scale invariance underlying the Kolmogorov 1941 picture. In a recent study of finite size effects, Dubrulle[10] showed that some properties of the structure functions (nonpower law behavior, nonlinear exponents, etc.) could be explained within a framework in which finite size cutoff plays a central role, and are felt throughout the so-called ''inertial range.'' Such finding is in clear contradiction with the ''local'' K41 theory, in which eddies in the inertial range are insensitive to the UV and IR end of the energy spectrum, and only interact with their neighbors (in the scale space) via ''local'' interactions (involving triads of comparable size). This observation motivated us to consider a new scenario for turbulence, in which anomalous corrections and deviations from Gaussianity are the results of *nonlocal interactions* between energy-containing structures. By nonlocal interactions, we mean interactions between well-separated scales (or highly elongated wave number triads). A numeri-

cal analysis on the role of the different triadic interactions in the energy cascade have previously been done by Brasseur *et al.*[11] and Domaradzki *et al.*[12] We have recently demonstrated via high-resolution numerical simulations that in two-dimensional (2-D) turbulence, the small-scale dynamics is essentially governed by their nonlocal interactions with the large scales.[13,14] This feature seems natural in view of the large-scale condensation of vortices.[15] As a result, the weak small scales are more influenced by the strong large-scale advection and shearing than by mutual interactions between themselves. This makes nonlocal interactions the dominant process at small scales.

2-D turbulence is very special, because there is no vortex stretching. As a result, there is no increase of vorticity toward smaller scales as is observed in 3-D turbulence. A quantitative feature underlying this difference is the shape of the energy spectra at small scales: it is k^{-3} in 2-D turbulence, much steeper than $k^{-5/3}$ 3-D energy spectra. In fact, a simple estimate shows that the borderline between local and nonlocal behaviors is precisely this k^{-3} spectrum: only for energy spectra steeper than k^{-3} can one prove rigorously than the dominant interactions are nonlocal. It is therefore not our intention to claim that 3-D turbulence is nonlocal, and in fact we do believe that local interactions are responsible for the $k^{-5/3}$ energy spectra. However, it is not unreasonable to think that evolution of the higher cumulants (responsible for deviations from Gaussianity at large deviations) is more nonlocal than it is for the energy spectrum. Indeed, calculation of higher cumulants in Fourier space involves integration over larger sets of wave numbers which (even if close in values pairwise) cover a larger range of scales than in the case of lower order cumulants.

A natural tool to study the role of the nonlocal interactions is the numerical simulation, because it allows a direct check of their influence by artificial switching-off of the elongated wave number triads in the Navier–Stokes equations or, on the contrary, retaining only such triads. A limitation of this approach lies in the restricted range of Reynolds number we are able to simulate. However, a recent comparison[16] showed that anomalous corrections and intermittency effects are quite insensitive to the Reynolds number. This shows the relevance of a low Reynolds number numerical study of intermittency. This approach is detailed in Sec. II, where we examine the dynamical role of the local interactions at the small scales using a simulation in which these interactions have been removed. We show that, as compared with a full simulation of the Navier–Stokes equations, such ''nonlocal'' simulation exhibits a flatter spectrum at small scales and stronger intermittency. As a qualitative indicator of intermittency we use plots of the vortex structures whose intensity greatly exceeds the rms vorticity value (''tornadoes'') and probability distribution function (PDF) plots, whereas to quantify intermittency we measure the structure function scaling exponents. We show that the main effect of the local interactions can be approximately described by a turbulent viscosity, while the nonlocal interactions are responsible for the development of the localized intense vortices and the deviations of Gaussianity. To validate that the enhanced intermittency is not merely a result of

the increased mean small-scale intensity (which could also be caused by some reason other than the nonlocality) we perform another numerical experiment in with the elongated triads were removed. Such ''local'' experiment resulted in even stronger small-scale intensity but the intermittency became clearly weaker. In Sec. III, we show how our findings can be used to provide both a qualitative estimate of the intermittency exponents, and a derivation of the Langevin equations for the velocity increments.

II. NONLOCAL INTERACTIONS IN 3-D TURBULENCE

A. The problematics

We consider the Navier–Stokes equations:

$$\partial_t \mathbf{u} + \mathbf{u} \cdot \nabla \mathbf{u} = -\nabla p + \nu \Delta \mathbf{u} + \mathbf{f}, \tag{1}$$

where u is the velocity, p is the pressure, ν is the molecular viscosity, and f is the forcing. In a typical situation, the forcing is provided by some boundary conditions (experiments) or externally fixed, e.g., by keeping a fixed low-wave-number Fourier mode at a constant amplitude (numerical simulation). This situation typically gives rise to quasi-Gaussian large-scale velocity fields, while smaller-scale velocities display increasingly non-Gaussian statistics. The presence of the forcing guarantees the existence of a stationary steady state in which the total energy is constant. In the absence of forcing, the turbulence energy decays steadily, due to losses through viscous effects. However, starting from a quasi-Gaussian large-scale field, one can still observe the development of increasingly non-Gaussian small scales in the early stage of the decay. We will study the effect of the nonlocal interactions on the statistics of such non-Gaussian small scales. For this, we introduce a filter function $G(\mathbf{x})$ in order to separate the large and small scales of the flow. In our numerical procedure, the filter G will be taken as a cutoff. We have checked that the results are insensitive to the choice of the filter, provided the latter decays fast enough at infinity. Using the filter, we decompose the velocity field into large scale and small scale components:

$$\mathbf{u}(\mathbf{x},t) = \mathbf{U}(\mathbf{x},t) + \mathbf{u}'(\mathbf{x},t),$$

$$\mathbf{U}(\mathbf{x},t) \equiv \overline{\mathbf{u}} = \int G(\mathbf{x}-\mathbf{x}') \mathbf{u}(\mathbf{x}',t) d\mathbf{x}'. \tag{2}$$

Equations for the large scales of motion are obtained by application of the spatial filter (2) to the individual terms of the basic equations (1). They are

$$\partial_j U_j = 0,$$

$$\partial_t U_i + \partial_j \overline{U_i U_j} + \partial_j \overline{U_i u_j + U_j u_i} + \partial_j \overline{u_i u_j}$$
$$= -\partial_i P + \nu \Delta U_i + F_i. \tag{3}$$

In these equations, we have dropped primes on subfilter components for simplicity; this means that from now on, any large-scale quantities are denoted by a capital letter, while the small-scale quantities are denoted by a lower case letter. The equation for the small-scale component is obtained by subtracting the large-scale equation from the basic equations (1); this gives

$$\partial_j u_j = 0,$$

$$\partial_t u_i + \partial_j ((U_i + u_i)(U_j + u_j) - \overline{(U_i + u_i)(U_j + u_j)})$$

$$= -\partial_i p + \nu \Delta u_i + f_i. \tag{4}$$

Several terms contribute to the interaction of scales: *nonlocal* terms, involving the product of a large scale and a small scale component, and a *local* term, involving two small-scale components. One way to study the dynamical effect of these contributions at small scales is to integrate numerically a set of two coupled equations, in which the local small scale interactions have been switched off at the small scales. (We do not switch off the local interactions at the large scales: this would hinder the cascade mechanism and prevent small scale generation from an initial large scale field.) This corresponds to the following set of equations:

$$\partial_t U_i + \partial_j \overline{U_i U_j} = -\partial_j \overline{U_i u_j} - \partial_j \overline{U_j u_i} - \partial_j \overline{u_i u_j} - \partial_i P$$
$$+ \nu \Delta U_i + f_i, \tag{5}$$

$$\partial_t u_i + \partial_j (U_i u_j) + \partial_j (u_i U_j) = -\partial_i p + \nu \Delta u_i + \sigma_i, \tag{6}$$

$$\partial_j U_j = \partial_j u_j = 0,$$

where

$$\sigma_i = \partial_j (\overline{U_i U_j} - U_i U_j + \overline{u_j U_i} + \overline{U_j u_i}). \tag{7}$$

The latter describes a forcing of the small scales by the large scales via the energy cascade mechanism. This term is always finite even when the external forcing **f** (which is always at large scales) is absent. The small scale equation is linear and it resembles the equations of the rapid distortion theory.[17] We shall therefore refer to this new model as the RDT model. The corresponding solution was then compared with a reference simulation performed at the same resolution, with the same initial condition. Note that this comparison is rather expensive numerically: Splitting the equations of motion between resolved and subfilter component leads to additional Fourier transforms, and increases the computational time by a factor of 3. This sets a practical limitation to the tests we could perform on our workstation. Also, an additional limitation came from the need of scale separation between the "large" and the "small" scales. This scale separation is mandatory in order to define "nonlocal" interactions. Their influence on anomalous scaling can be checked only if the typical small scale lies within the inertial range. For this reason, we were led to consider a situation of decaying (unforced) 3-D turbulence, with a flat energy spectrum at large scale, and an "inertial range" mostly concentrated at small to medium scales ($10 < k < 40$ for a 256^3 simulation). Indeed, at the resolution we could achieve, forced turbulence developed an inertial range of scale around $k = 8$, too small for the scale separation to be effective [see Ref. 18 for a study and discussion of this case and its relevance to large eddy simulations (LES)]. Decaying turbulence does not, by definition, achieve a statistically stationary state, with mathematically well-defined stationary probability distribution functions (PDFs). Therefore, all the PDFs were computed at a fixed time which we have chosen to be at the end of each simulation (at $t = 0.48$).
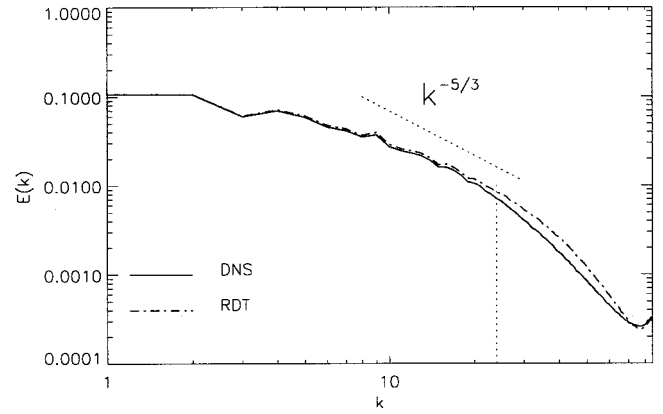

FIG. 1. Comparison of energy spectra at $t = 0.48$ obtained via the DNS and the RDT simulation.

B. The numerical procedure

1. The numerical code

Both the Navier–Stokes equation (1) and the set of RDT equations (6) were integrated with a pseudospectral code (see Ref. 2 for more details on the code). In the RDT case, a sharp cutoff in Fourier space was used to split the velocity field into large- and small-scale components in Fourier space and all nonlinear terms were computed separately in the physical space. The aliasing was removed by keeping only the 2/3 largest modes corresponding to the 85 first modes in our case. The calculations presented here were done with 256^3 Fourier modes and a viscosity of 1.5×10^{-3} corresponding to a Reynolds number $57 < R_\lambda < 80$ (where R_λ is the Reynolds number based on the Taylor microscale λ).

2. The simulations

The test was performed in a situation of decaying turbulence where the forcing term f_i is set to zero. We performed several different simulations: a direct numerical simulation (DNS), a RDT simulation [Eq. (6)], and a "local" experiment (see the end of this section). In all cases, the initial condition was chosen as the output of a preliminary simulation of an initially Gaussian velocity field over several turnover times. In order to allow enough energy at the large scales, the sharp cutoff filter was taken at the wave number $k = 24$ corresponding to approximately five Kolmogorov scales. Because of the very low speed of the RDT simulation (three times more expensive than the DNS) the two simulations were performed between $t = 0$ and $t = 0.48$ corresponding to approximately 2.5 turnover times.

C. Comparison of the RDT and DNS experiments

1. Spectra

The comparison of spectra is shown in Fig. 1. In the DNS case, one observes a classical evolution, in which the large scale energy decays while the inertial $k^{-5/3}$ range tends to move toward smaller scales. It can be seen that the inertial range (characterized by the $-5/3$ slope) only marginally exists. In the RDT case, one observes a similar evolution at large scale, while a tendency toward a flatter spectrum is
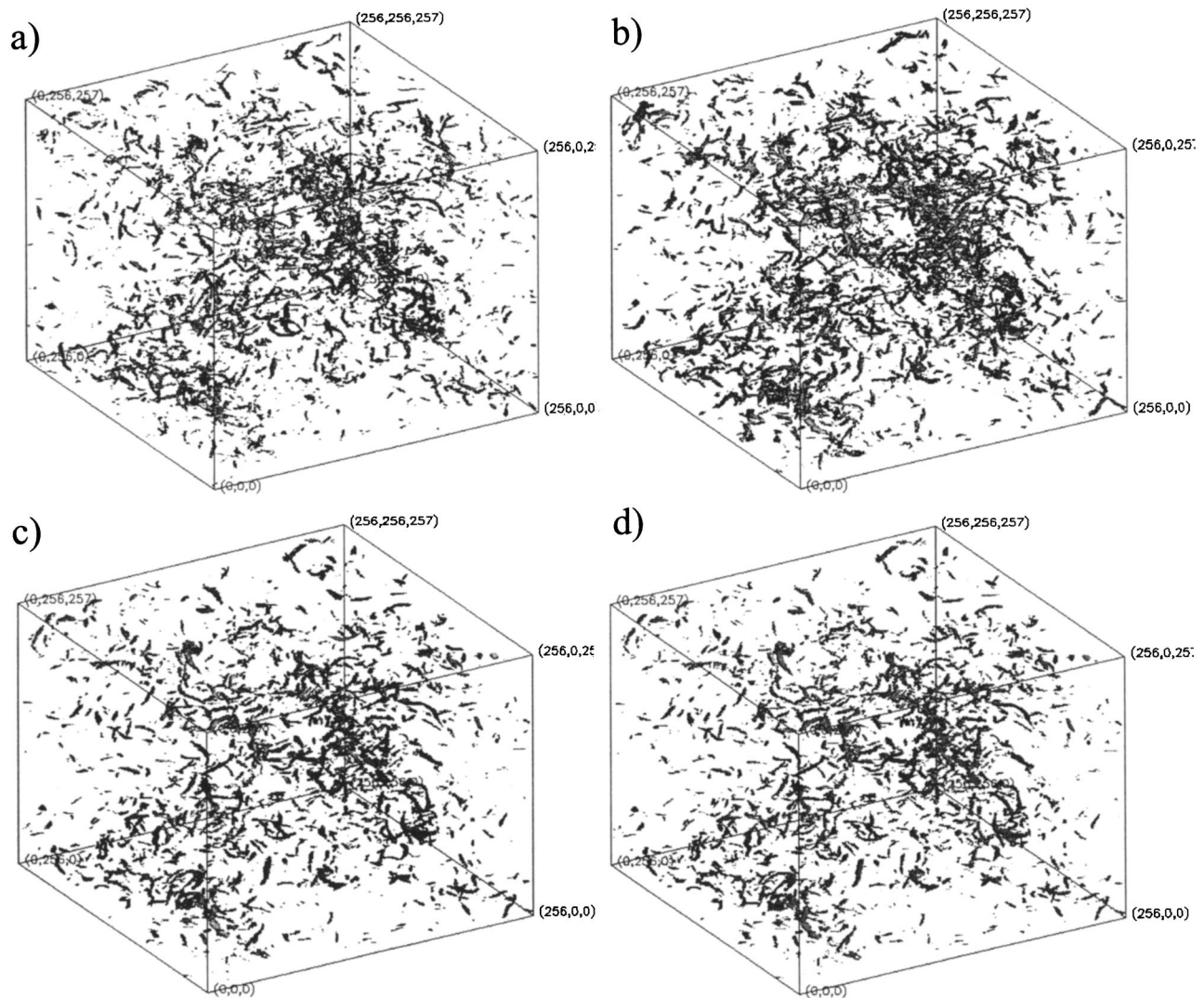
FIG. 2. Comparison of vortex structures (isoplot of vorticity $|\omega| = 3.5\omega_{rms} = \omega_c$ at $t = 0.48$) for (a) DNS, (b) RDT, (c) RDT+constant turbulent viscosity, (d) RDT+the RNG-type turbulent viscosity. The number of ''tornadoes'' estimated by $N = \int_{\omega_c}^{\infty} PDF(|\omega|)d\omega$ are, respectively, 8245 (a), 21 669 (b), 10 226 (c), and 10 779 (d).

observed near and beyond the separating scale (beyond which local interactions are ignored). We checked that this behavior is not sensitive to the resolution.

The range of computed scales is insufficient to find a reliable value of the spectral slope in the RDT case. However, this slope can be predicted by a simple dimensional argument. This argument was presented for the 2-D case in Ref. 19, but it is essentially the same for 3-D. Indeed, in the RDT case the small-scale equations are linear and, therefore, the energy spectrum $E(k)$ must be linearly proportional to the energy dissipation rate, ϵ. In this case, the only extra dimensional parameter (in comparison with the local/ Kolmogorov case) is the large-scale rate of strain α. There is the only dimensional combination of ϵ, α and wave number k that has the dimension of $E(k)$; this gives

$$E_k = \frac{C\epsilon}{\alpha} k^{-1}, \tag{8}$$

where C is a nondimensional constant. In our case, our resolution is too low to be able to check whether the RDT spec-

trum follows a k^{-1} law, but we clearly see the tendency to a flatter than $-5/3$ slope. The RDT case is reminiscent of the boundary layer in which a k^{-1} spectra have been observed.[20] This is not surprising because the presence of the mean shear increases the nonlocality of the scale interactions corresponding to RDT. In fact, an exact RDT analysis of the shear flow does predict formation of the k^{-1} spectrum.[21]

2. Structures

3-D turbulence is characterized by intense thin vortex filaments (''tornadoes'').[1–3,22] Their radii are of order of the dissipative (Kolmogorov) scale, which in this case is determined by the balance of the large-scale straining and viscous spreading. In this respect, these vortices are similar to the classical Burgers vortex solution. Figure 2 shows a comparison of the ''tornadoes'' observed in the DNS and in the RDT, which are visualized by plotting surfaces of strong vorticity ($|\omega| > 3.5\omega_{rms}$). In both cases, thin filamentary structures are observed, but they appear to be much more
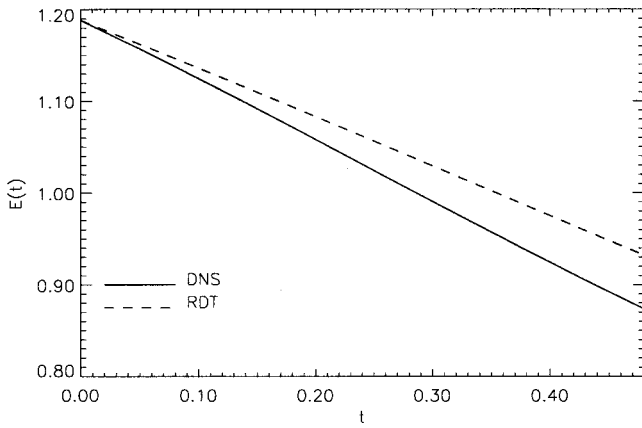
FIG. 3. Comparison of the time evolution of total energy.

FIG. 5. Time evolution of total energy obtained via the DNS and the RDT simulation with the two different turbulent viscosities.

numerous in the RDT case. Obviously, local interactions tend to dissipate the ''tornadoes,'' which can be interpreted as a mutual distortion and entanglement of ''tornadoes,'' preventing their further stretching by the large scales. On the macroscopic level, this can be regarded as an additional, ''turbulent,'' viscosity produced by the local interactions. This is compatible with the flattening of the energy spectrum in the RDT case, which we interpreted previously in terms of the turbulent viscosity effect.

It is interesting that the Burgers vortex is essentially a linear solution because of the cylindrical shape of this vortex, which prevents the appearance of the quadratic (in vorticity) terms. Such a linearity is a typical feature of all RDT solutions. On the other hand, there is another candidate which has often been considered to be responsible for intermittency: this is a vortex reconnection process which is believed to lead to a finite time singularity formation (at least for inviscid fluids). Note that the vortex reconnection is an essentially nonlinear process in which the local scale interactions are playing an important role and cannot be ignored. Indeed, there is no finite time blow-up solutions in linear RDT. Likewise, the vorticity grows only exponentially in the Burgers vortex and it does not blow up in a finite time. From this perspective, our numerical results show that the local (vortex–vortex) interactions mostly lead to destruction of the intense vortices and prevention of their further Burgers-like
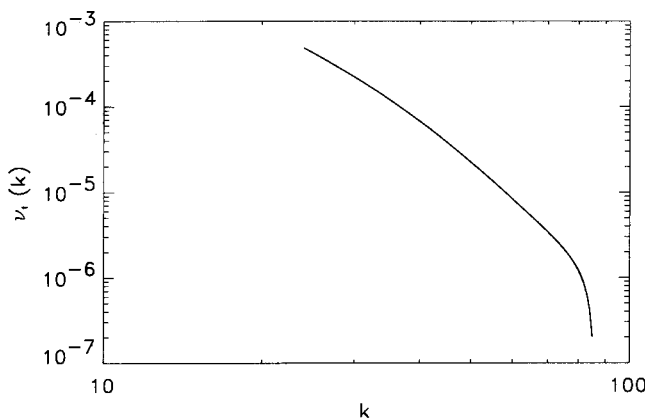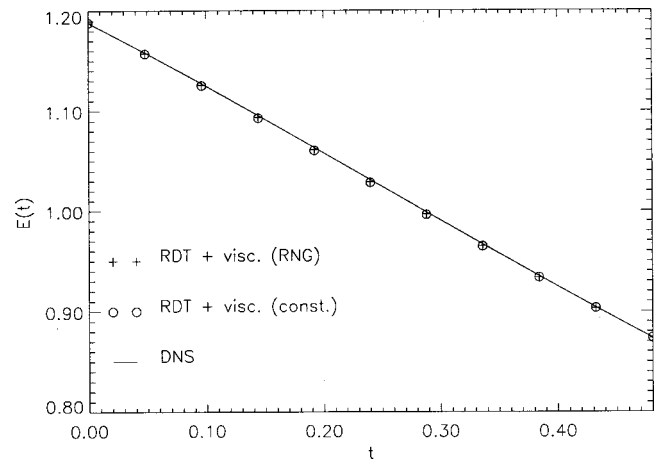
(exponential) growth which has a negative effect on the intermittency. This process seems to overpower the positive effect of the local interactions on the intermittency which is related to the reconnection blow-ups. At the moment, it is not possible to say if the same is true for much higher Reynolds number flows.

3. Turbulent viscosity

Comparison of the DNS and RDT results for the time evolution of the total energy is shown in Fig. 3. One clearly observes a slower decline of the total energy in the RDT case, as if there was a lower viscosity. This result is not surprising: It is well known that the influence of energy motions onto well separated large scales (see Refs. 23–25 for systematic expansions) is through an effective eddy viscosity, supplied by the $\langle uu \rangle$ term. Our result suggests that, to a first approximation, the difference between the RDT and the DNS could be removed by including an additional ''turbulent'' viscosity in the RDT simulation. For the sake of simplicity, we decided to choose an isotropic tensor, chosen as to conserve the total energy. We tried two simple viscosity prescriptions: one in which ν_t is constant, and one (Fig. 4) in

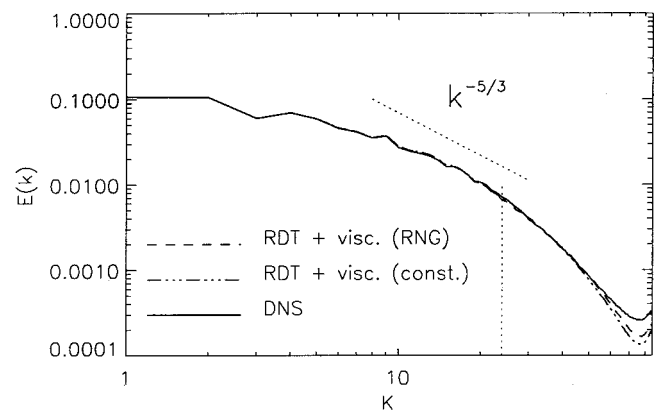FIG. 4. Spectrum of the turbulent viscosity computed by (9) at $t = 0.48$.

FIG. 6. Comparison of energy spectra obtained via the DNS and the RDT simulation with two different forms of the turbulent viscosity.
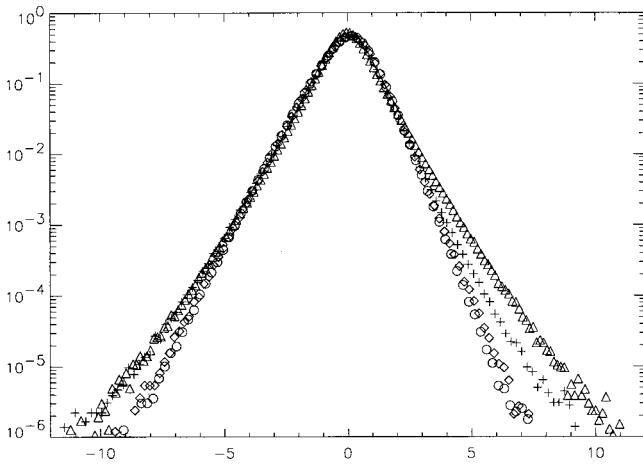
FIG. 7. Comparison of the PDF of the longitudinal velocity increments defined by Eq. (10) for $\ell=2\pi/256$ (5×10^7 statistics at $t=0.48$ for the velocity field from the four simulations): DNS (circle), RDT (crosses), RDT+constant viscosity (diamonds), and RDT+viscosity computed from RNG (triangles).

which the viscosity prescription follows the shape dictated by renormalization group theory (RNG) (see, e.g., Ref. 26):

$$\nu_t(k)=\left(\nu^2+A\int_k^{+\infty}q^{-2}E(q)dq\right)^{1/2}-\nu. \tag{9}$$

The constants were adjusted so as to obtain a correct energy decay (Fig. 5). They are $\nu_t=0.0002$ for the constant ν_t prescription, and $A=0.02$ for the other one. We elaborate more on the choice of this turbulent viscosity in Sec. III C. Yet another method we tried was to replace the neglected nonlinear term (interaction of small scales among themselves) with its mean value. Dividing this mean nonlinear term by k^2 for each k one can compute the turbulent viscosity $\nu_t(k)$. The result is interesting: ν_t turns out to be nearly independent of k; this provides an extra justification for the simple model in which $\nu_t=$ const.

The energy spectra and energy decay obtained with this new RDT simulation are shown in Figs. 6 and 5. One sees that one now captures exactly the energy decay of the DNS.
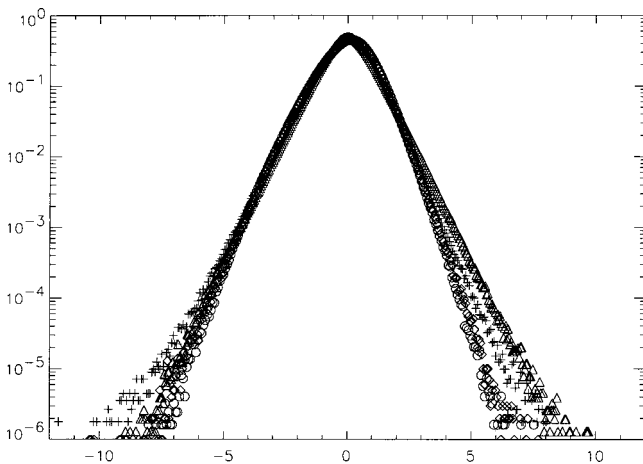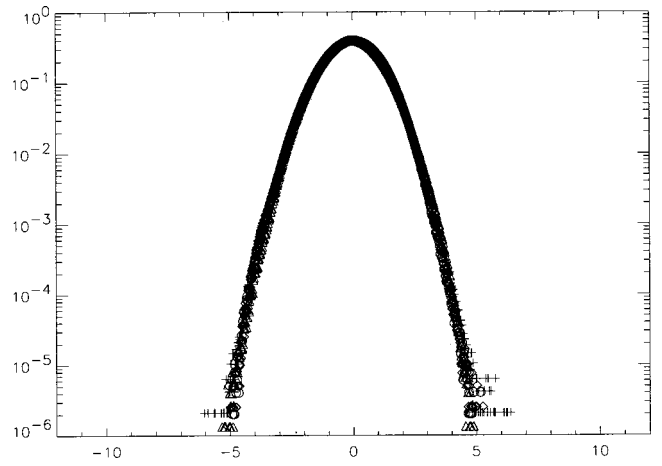

FIG. 8. Same as Fig. 7 for $\ell=2\pi/64$.

FIG. 9. Same as Fig. 7 for $\ell=2\pi/4$.

The energy spectra become closer to the DNS result at low and intermediate k, whereas at the high k they depart from DNS indicating an overdissipation of the smallest scales. The latter is an artifact of our crude choice for the turbulent viscosity ignoring its anisotropy and possibility for it to take negative values. The turbulent viscosity also influences the anomalous corrections, as we will now show it.

4. PDFs and exponents

We conducted a statistical study of our velocity fields corresponding to the end of the simulations ($t=0.48$). As usual for the study of the anomalous properties of turbulence, we consider the velocity increments over a distance $\mathbf{l}$,

$$\delta\mathbf{u_l}=\mathbf{u}(\mathbf{x}+\mathbf{l})-\mathbf{u}(\mathbf{x}). \tag{10}$$

As usual, we will deal with the longitudinal and transverse to $\mathbf{l}$ velocity increments, $\delta u_{l\parallel}=(\delta\mathbf{u_l}\cdot\mathbf{l})/\mathbf{l}$ and $\delta u_{l\perp}=(\delta\mathbf{u_l}\times\mathbf{l})/\mathbf{l}$, respectively, where $l=|\mathbf{l}|$. Figures 7–9 show the probability distribution functions (PDFs) of the longitudinal
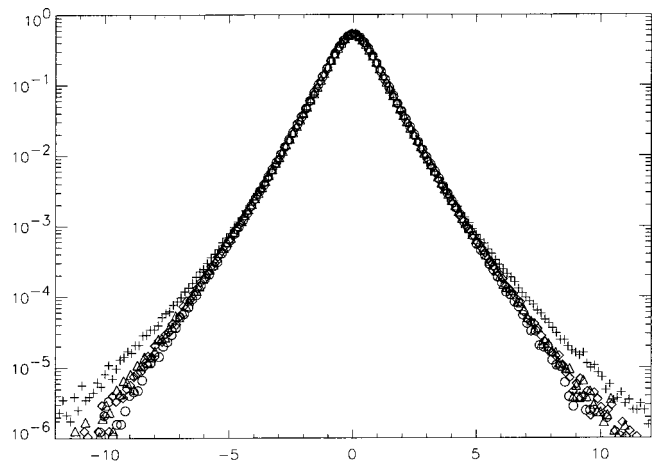

FIG. 10. Comparison of the PDF of the transverse velocity increments defined by Eq. (10) for $\ell=2\pi/256$ (5×10^7 statistics at $t=0.48$ for the velocity field from the four simulations): DNS (circles), RDT (crosses), RDT+constant viscosity (diamonds), and RDT+viscosity computed from RNG (triangles).
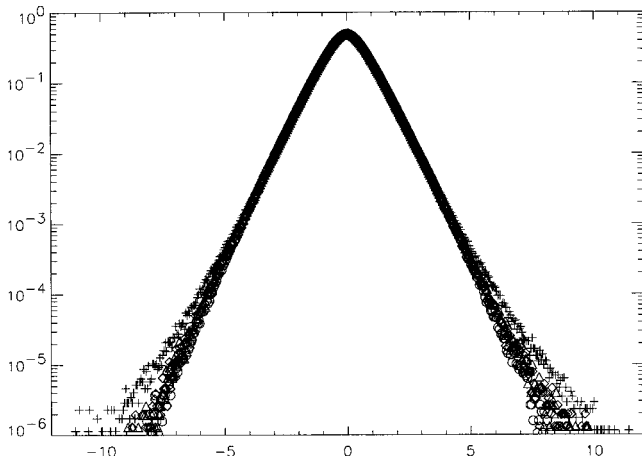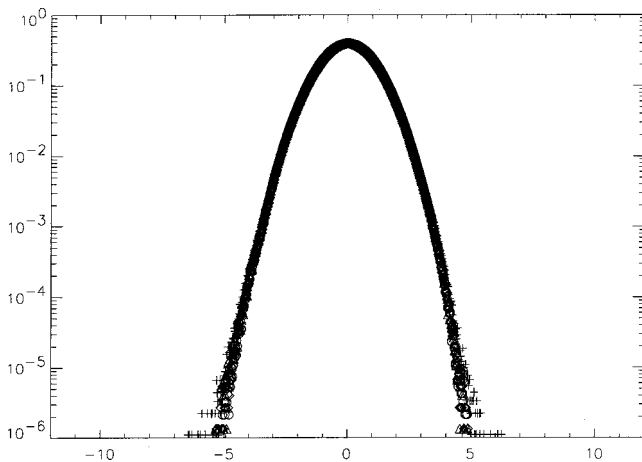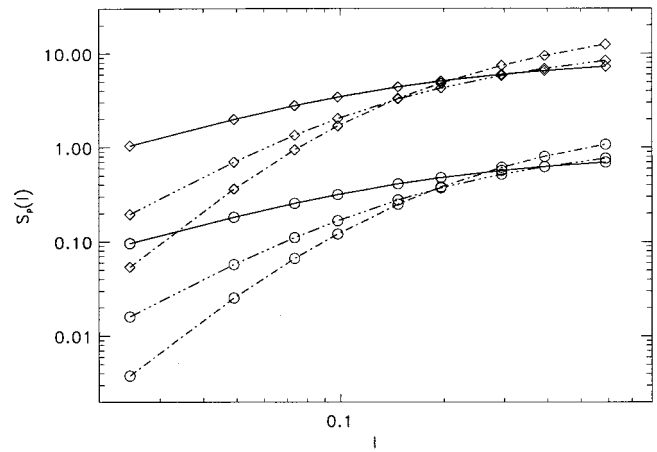
FIG. 11. Same as Fig. 10 for $\ell = 2\pi/64$.

FIG. 13. Structure functions computed with the PDF of the longitudinal velocity increments from DNS (circles) and the RDT (diamonds) for the first (solid line), second (dash-dotted line), and third (dash-dot-dot line) moments (for convenience of presentation, the RDT structure functions have been multiplied by 10).

increments and Figs. 10–12 the PDFs of transverse increments, for three values of l, obtained by the DNS, and our different RDT simulation (with and without turbulent viscosity). At large scale, one observes a quasi-Gaussian behavior, with the development of wider tails as one goes toward smaller, inertial scales. This widening of the PDFs is a classical signature of the anomalous scaling observed in turbulence. It can be measured by studying the scaling properties of the velocity structure functions,

$$S_p(\ell) = \langle \delta u_\ell^p \rangle. \tag{11}$$

In the inertial range, the structure function vary like ℓ^{ζ_p}. For low Reynolds number turbulent flows, the scaling behavior in the inertial range is very weak or undetectable because the inertial range is very short. To exemplify this point, we show in Figs. 13 and 14 the structure functions as a function of the scale separation for the longitudinal and the transverse velocity increments (the structure functions from the RDT simulation were shifted by a factor of 10 for the clarity of the figures). Given the very weak scaling of our structure functions, we may use the extended self-similarity (ESS) property,[27] which states that $S_p(\ell) \sim S_3^{\zeta_{p/\zeta_3}}$ even outside the inertial range of scales. We use this property because it al-

lows one to find the scaling exponents in a more unambiguous way.[27] The measured exponents in our DNS are shown in Fig. 15 and in Table I. In both the longitudinal and transverse cases, they are in agreement with the previously reported relative exponents[16] and they display a clear deviation from the "nonintermittent" value $\zeta_p = p/3$. Note that measurements in the atmospheric boundary layer seem to indicate that the transverse third-order scaling exponent is less than one.[28] We cannot check this directly in our low Reynolds number DNS, but observe that this leads to a larger difference between relative transverse and longitudinal exponents than the difference between real exponents observed by Dhruva et al.[28] and Camussi et al.[29] Corresponding quantities for the RDT simulation are shown in Fig. 15 and Table I. One sees that the RDT statistics display larger and more intermittent PDF tails for small scales, which makes the scaling exponents take smaller values corresponding to larger anomalous corrections. Again, this situation is reminiscent of the case of the boundary layer. In fact, the measured values in our simulation are remarkably similar to those reported in the atmospheric boundary layer[28] (after the correction taking

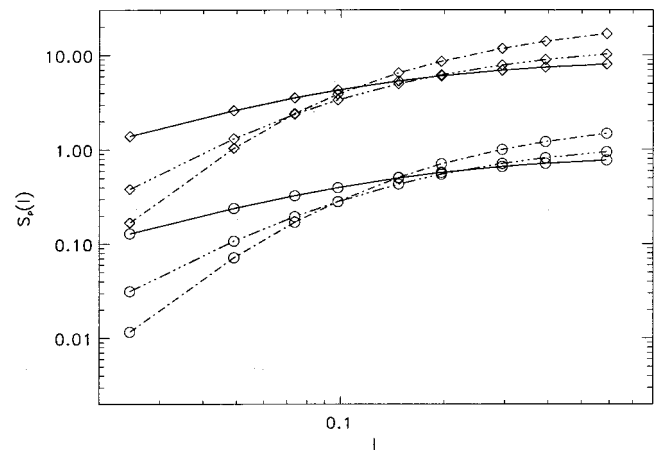FIG. 12. Same as Fig. 10 for $\ell = 2\pi/4$.

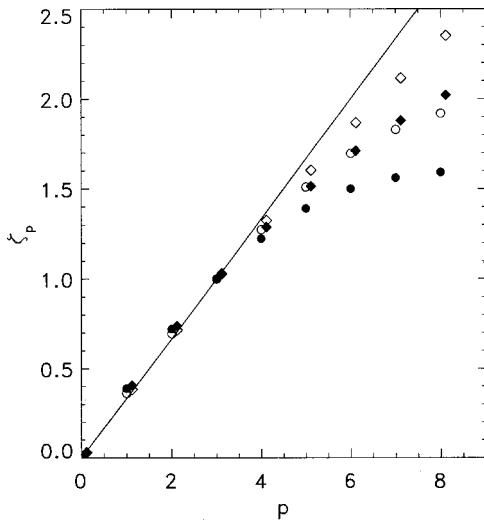FIG. 14. Same as Fig. 13 for the transverse velocity increments.

FIG. 15. Comparison of the scaling exponents computed from the DNS (diamonds) and the RDT (circles) statistics. The longitudinal exponents are plotted with open symbols and the transverse exponents with closed symbols.

TABLE II. Scaling exponents of the velocity structure functions from: atmospheric turbulence at $10\,000 < R_\lambda < 15\,000$ [Dhruva *et al.* (Ref. 28)] channel flow [Toschi *et al.* (Ref. 31)] near the wall ($20 < y^+ < 50$) and far from the wall ($y^+ > 100$) at Re=3000 and boundary layer at $R_\delta = 32\,000$ [Zubair (Refs. 30 and 51)].

	Longitudinal				Transverse
Order	Dhruva	Zubair	Toschi $20 < y^+ < 50$	Toschi $y^+ > 100$	Dhruva
1	0.366	⋯	0.44	0.37	0.359
2	0.700	0.70	0.77	0.70	0.680
3	1.000	1.00	1.00	1.00	0.960
4	1.266	1.20	1.17	1.28	1.200
5	1.493	1.52	1.31	1.54	1.402
6	1.692	1.62	1.44	1.78	1.567
7	⋯	1.96	1.55	2.00	⋯

into account the fact that we measure exponents relative to ζ_3) or in a turbulent boundary layer.[30] They are in between the two different values measured by Toschi (Ref. 31) in and above the logarithmic layer in numerical DNS of a channel flow. A summary of these results is given in Table II. When a turbulent viscosity is added to the RDT simulation, the intermittent wings are less pronounced in the PDFs and the anomalous correction decreases (Table I), becoming similar to those observed in the DNS. This agrees with the picture in which the anomalous corrections are determined by the nonlocal interactions, while the local interactions act to restore the classical Gaussian (Kolmogorov-like) behavior. Obviously, the shape of the turbulent viscosity also influences the intermittency correction: For the transverse case, where there is no asymmetry of the PDFs, both the constant turbulent

TABLE I. Scaling exponent of the velocity structure functions measured using the ESS property, in various simulations, at $t=0.48$.

Order	K41	DNS	RDT	RDT+Visc. 1	RDT+Visc. 2	Local
			Longitudinal			
1	0.333	0.353	0.361	0.353	0.354	0.344
2	0.667	0.687	0.695	0.687	0.687	0.678
3	1.0	1.0	1.0	1.0	1.0	1.0
4	1.333	1.295	1.273	1.294	1.293	1.310
5	1.667	1.573	1.509	1.570	1.568	1.607
6	2.0	1.836	1.696	1.830	1.824	1.892
7	2.333	2.085	1.828	2.073	2.064	2.164
8	2.667	2.321	1.919	2.301	2.287	2.423
			Transverse			
1	0.333	0.375	0.388	0.376	0.376	0.352
2	0.667	0.707	0.721	0.708	0.709	0.685
3	1.0	1.0	1.0	1.0	1.0	1.0
4	1.333	1.258	1.223	1.255	1.253	1.297
5	1.667	1.484	1.390	1.477	1.468	1.578
6	2.0	1.680	1.499	1.664	1.645	1.843
7	2.333	1.849	1.560	1.822	1.782	2.094
8	2.667	1.991	1.591	1.952	1.882	2.333

viscosity and the RNG turbulent viscosity provide intermittency corrections which are of the same level as the DNS. This is quite remarkable, since they include only one adjustable parameter, tuned as to conserve the total energy. For the longitudinal case, where an asymmetry is present, the two prescriptions give noticeably different results: As one goes toward lower scales, and as the asymmetry becomes larger between the positive and the negative increments, the PDFs computed with RDT and constant turbulent viscosity display tails which are very close to that of DNS, while the PDFs of the RDT with turbulent RNG viscosity have a tendency toward a symmetrical shape, thereby failing to reproduce the DNS behavior. This difference of behavior between the RNG and constant turbulent viscosity will be further investigated in Sec. III.

D. Comparison of the ''local'' experiment with DNS

Given the comparison of the DNS and the RDT (''nonlocal'') simulations, one could argue that the increase of the intermittency in RDT is mostly due to the increased mean intensity of the small scales (which is seen on the energy spectrum plot). A similar increase of the small-scale intensity could be produced by other means which have nothing to do with nonlocality, e.g., by reducing viscosity in DNS. Will there be stronger intermittency in all such cases too? In order to prove that it is not the case, we perform a simulation where, as the opposite of the RDT one, the nonlocal interactions at small scales were removed from the Navier–Stokes (NS) equation and only the local interactions were retained. In order to keep the local interactions which involve scales close to the cutoff scales, the velocity and the vorticity fields were split into three parts: the large scales, the medium scales near the cutoff, and the small scales. This decomposition is defined in Fourier space as follows:

$$\mathbf{u}(\mathbf{k}) = \mathbf{u}_{ls}(\mathbf{k}) + \mathbf{u}_{ms}(\mathbf{k}) + \mathbf{u}_{ss}(\mathbf{k}), \tag{12}$$

$$\omega(\mathbf{k}) = \omega_{ls}(\mathbf{k}) + \omega_{ms}(\mathbf{k}) + \omega_{ss}(\mathbf{k}), \tag{13}$$

where

Phys. Fluids, Vol. 13, No. 7, July 2001
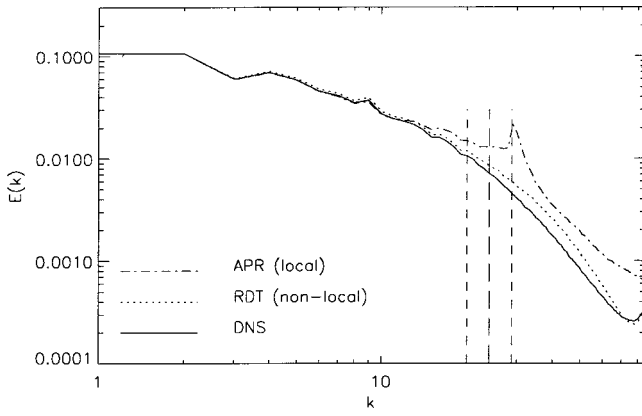
Nonlocality and intermittency in 3-D turbulence   2003

FIG. 16. Comparison of energy spectra obtained via the DNS, RDT, and the ''local'' simulation at $t=0.48$.

$$\mathbf{u}_{ls}(\mathbf{k})=\mathbf{u}(\mathbf{k})\quad\text{for }k<k_c/C$$
$$=0\quad\text{for }k>k_c/C,$$
$$\mathbf{u}_{ms}(\mathbf{k})=\mathbf{u}(\mathbf{k})\quad\text{for }k_c/C<k<Ck_c$$
$$=0\quad\text{for }k_c/C<k\text{ and }k>Ck_c,\qquad(14)$$
$$u_{ss}(k)=u(k)\quad\text{for }Ck_c<k$$
$$=0\quad\text{for }k>Ck_c.$$

Using these definitions, the equation for the ''local'' simulation was the following:

$$\partial_t\mathbf{u}(\mathbf{k})+P(\mathbf{u}\cdot\nabla\omega)(\mathbf{k})-[P(\mathbf{u}_{ls}\cdot\nabla\omega_{ss})(\mathbf{k})$$
$$+P(\mathbf{u}_{ss}\cdot\nabla\omega_{ls})(\mathbf{k})]_{\{k>k_c\}}=\nu\Delta\mathbf{u}(\mathbf{k}),\qquad(15)$$

where P is the projector operator defined by $P_{ij}=\delta_{ij}-k_ik_j/k^2$. In our simulation we choose $C=1.2$ and the same cutoff scale $k_c=24$. The results of this simulation are compared to the equivalent results from the DNS and the RDT simulation. The energy spectra are compared in Fig. 16. This ''local'' simulation contains more energy at small scales than the DNS and even the RDT. The bump of energy near the cutoff scale k_c is due to the fact that the ''local'' approximation is introduced only for scales smaller than k_c. Despite the high level of energy at small scales, the solution of this ''local'' simulation is much less intermittent than the equivalent field from DNS and RDT. A comparison of the scaling exponents is shown Fig. 17 and Table I for both the longitudinal and transverse velocity increments. These results confirm the idea that intermittency is caused by the nonlocal interactions and not just by the mere presence of the small scales.

III. QUALITATIVE EXPLANATION OF THE INTERMITTENCY

Our results can be used to get a qualitative understanding of the intermittency via the scale behavior of both the PDF of the velocity increments and its moments. For this, we are going to build a new model of turbulence, mimicking the small scale nonlocal dynamics. In spirit, this amounts to an ''antishell'' model of turbulence, because, here, we retain
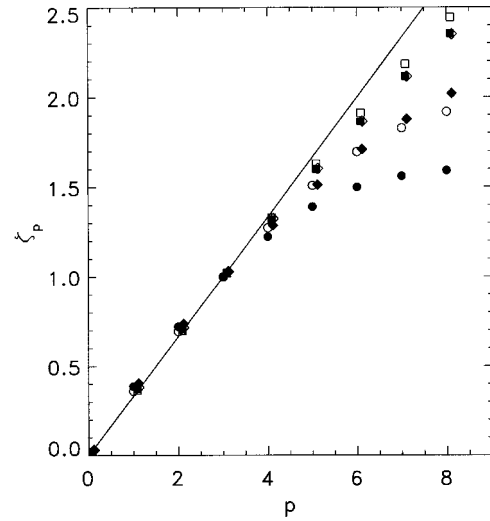

FIG. 17. Comparison of the scaling exponents computed from the DNS (diamonds), RDT (circles), and the ''local'' simulation (squares) statistics. The longitudinal exponents are plotted with open symbols and the transverse exponents with closed symbols.

only interactions between distant wave numbers, by contrast with the ordinary shell model[32–34] which theoretically only retains local interactions. In this context, it is interesting to note that the ordinary shell model requires a certain degree of nonlocality between modes so as to generate intermittency: It can indeed be proven that the intermittency correction disappears when the separation between two consecutive shell tends to zero.[35] Another known pitfall of the shell model is its incapacity to describe the observed skewness (asymmetry) generation along the scale of the PDF of the longitudinal increments. This is annoying, since this skewness is directly related to the nonzero value of the third-order moment, and, hence, to the essence of the Kolmogorov cascade picture via the 4/5 law. Finally, the original shell model is very crude, since there is no spatial structure (everything is described by Fourier modes). We now show how elaborate a cleaner model of turbulence using localized wave packets, leading to a description of the small-scale statistics in term of Langevin processes subject to coupled multiplicative and additive noise.

A. The Langevin model of turbulence

Our numerical simulations showed that both the energy spectrum (and decay) and the intermittency quantities are well reproduced by a model in which only the nonlocal interactions are left in the small-scale equations whereas the local interactions of small scales among themselves are replaced by a turbulent viscosity term. Such a model is described by Eq. (6) with ν replaced by the turbulent viscosity coefficient ν_t in the small-scale equations,

$$\partial_t u_i+\partial_j(U_iu_j)+\partial_j(u_iU_j)=-\partial_ip+\nu_t\Delta u_i+\sigma_i,$$
$$\partial_ju_j=0,\qquad(16)$$

and σ_i is given by (7). We are interested in the contribution of nonlocal interactions to the statistics of the non-Gaussian small scales. For this, we assume that the large scale (L)

quantities ($\mathbf{U}$ and its derivative, and σ_i) are fixed external processes, with prescribed statistics (to be defined later), and derive an equation for the small scale $\mathbf{l}$ velocity field $\mathbf{u}'$, by taking into account the scale separation $\ell/L = \epsilon \ll 1$. For this, we decompose the velocity field into localized wave packets via a Gabor transform (GT) (see Ref. 36)

$$\hat{u}(\mathbf{x},\mathbf{k},t) = \int g(\epsilon_* |\mathbf{x}-\mathbf{x}'|) e^{i\mathbf{k}\cdot(\mathbf{x}-\mathbf{x}')} \mathbf{u}(\mathbf{x}',t) d\mathbf{x}', \qquad (17)$$

where g is a function which decreases rapidly at infinity and $1 \ll \epsilon_* \ll \epsilon$. Note that the GT of $\mathbf{u}$ is a natural quantity for the description of the velocity increments because of the following relation:

$$\mathbf{u}(\mathbf{x}+\mathbf{l}) - \mathbf{u}(\mathbf{x}-\mathbf{l}) = \frac{1}{2i} \int e^{-\mathbf{l}\cdot\mathbf{k}} \operatorname{Im} \hat{\mathbf{u}}(\mathbf{x},\mathbf{k}) dk. \qquad (18)$$

Thus, velocity increments are related to GT via the Fourier transform, and all information about the l dependence is contained in the GT dependence on k (the main contribution to the above-mentioned integral comes from $k \sim 2\pi/l$). On purely dimensional ground, we see that $\hat{u} \sim k^{-d} \delta u$, where d is the dimension. Therefore, in the sequel, we shall identify $k^d \operatorname{Im} \hat{u}$ with the velocity increment.

Applying GT to (6) we have (see Ref. 37 for details)

$$D_t \hat{\mathbf{u}} = \hat{\mathbf{u}} \cdot \hat{\boldsymbol{\xi}} + \hat{\sigma}_\perp - \nu_t k^2 \hat{\mathbf{u}}, \qquad (19)$$

where ξ and $\sigma_\perp$ are random processes, given by

$$\hat{\boldsymbol{\xi}} = \boldsymbol{\nabla} \left(2 \frac{\mathbf{k}}{k^2} \mathbf{U} \cdot \mathbf{k} - \mathbf{U} \right),$$
$$\hat{\sigma}_\perp = \hat{\sigma} - \frac{\mathbf{k}}{k^2} (\mathbf{k} \cdot \hat{\sigma}), \qquad (20)$$

and

$$D_t = \partial_t + \dot{\mathbf{x}} \cdot \boldsymbol{\nabla} + \dot{\mathbf{k}} \cdot \boldsymbol{\nabla}_\mathbf{k}, \qquad (21)$$
$$\dot{\mathbf{x}} = \mathbf{U} = \boldsymbol{\nabla}_k H,$$
$$\dot{\mathbf{k}} = -\boldsymbol{\nabla}(\mathbf{k} \cdot \mathbf{U}) = -\boldsymbol{\nabla} H, \qquad (22)$$
$$H = \mathbf{U} \cdot \mathbf{k}. \qquad (23)$$

Because the large-scale dynamics is local in k space, it is only weakly affected by the small scales and the quantities ξ and σ in Eq. (19) can be considered as a given noise. Also, because the equation is linear in $\hat{u}$, we immediately see that $k^d \hat{u}$ will also satisfy an equation similar to (19) subject to a straightforward modification of the force definitions. Before elaborating more on (19), it is convenient to study in closer detail the physical parameters of this equation.

B. The noises

In Eq. (19), the noise ξ and $\sigma_\perp$ appears as the projector of two quantities, one related to the velocity derivative tensor, and another related to the Gabor transform of the energy transfer from large to small scales. In the sequel, we present a statistical study of these two noises in physical space (i.e., after inverse Gabor transforming $\hat{\sigma}_\perp$). We will also consider the Fourier spectra of the corresponding two-point correla-
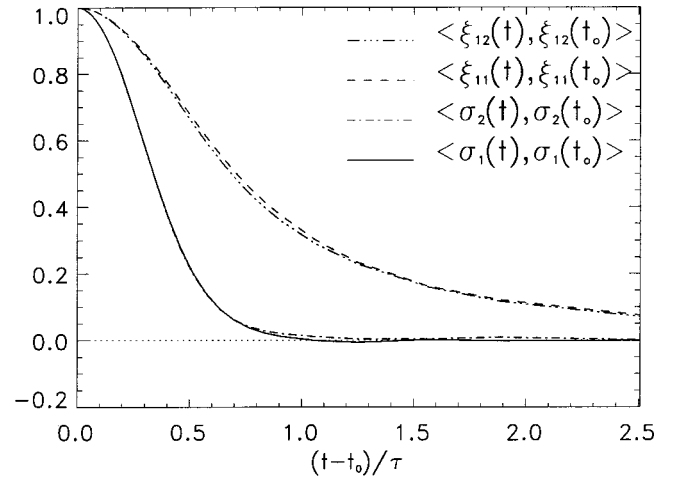

FIG. 18. The normalized autocorrelation in time for the two force components σ and ξ (the turnover time τ is equal to 0.19).

tions. Let us choose $\mathbf{k}$ to be along one of the coordinate axes (without loss of generality because of the isotropy). Then the components of ξ coincide (up to the sign) with the corresponding components of the velocity derivative tensor, and we will use this fact in the rest of this section. The velocity derivative tensor has been studied in the literature, e.g., in Refs. 38 and 39, in terms of correlations between the directions of the antisymmetrical part of the tensor (the vorticity) and the symmetrical part (the strain). Over a long time, the vorticity appears to be aligned with the direction of largest stretching. Other studies focused on the PDF of the modulus of one component. For example, Marcq and Naert[40] observe that the derivative has a highly non-Gaussain distribution, but with a correlation function which decays rapidly, and can be approximated by a delta function at scales large compared to the dissipative scale. In the present case, we observe different features. Because of the isotropy, we can concentrate only on two quantities, say ξ_{11} and ξ_{12}. Figure 18 shows the equal-position, time correlation $C_{1i}(t-t_0) = \langle \xi_{1i}(t)\xi_{1i}(t_0) \rangle$ and $\alpha_{ii}(t-t_0) = \langle \sigma_i(t)\sigma_i(t_0) \rangle$ as a function of $t-t_0$. Note that these quantities are normalized to 1 at $t=t_0$ in Fig. 18. First, we see that C_{11} approximately coincides with C_{12} and α_{11} coincides with α_{22}, which is a good indicator of isotropy (without normalization there would be $C_{12} = -3C_{11}$). Second, we see that the correlation C_{11} and C_{12} decay to zero over a time scale which is of the order of few turnover times τ ($\tau=0.19$). On the other hand, the correlation of σ decay much faster, over a time of the order of $\tau/2$. Figure 19 displays the Fourier transforms of the equal-time two-point correlation $D_{1i}(x-x_0) = \langle \xi_{1i}(x,y,z,t)\xi_{1i}(x_0,y,z,t) \rangle$ and $\alpha_{ii}(x-x_0) = \langle \sigma_i(x,t)\sigma_i(x_0,t) \rangle$. One sees that all correlations are very weak beyond $2k_c$. The correlation D_{12} appears to be the largest at large scales, but it decays more rapidly than the other correlations. We have also investigated the cross correlations between the noises. The equal position cross correlations are displayed in Fig. 20. The correlation is rather weak, but there is a tendency for σ_i to be correlated with ξ_{1i} over a time scale of the order of τ, while it is anticorrelated with the other component of the tensor, over such a time scale. The equal time correlations are shown in Fig. 21. No-
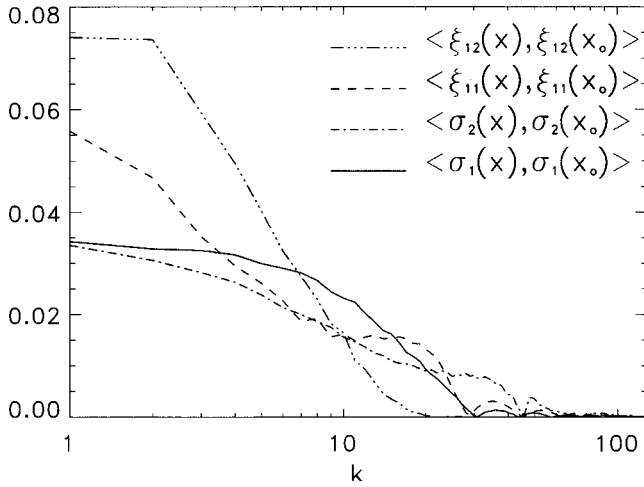
FIG. 19. Fourier transform of the space autocorrelation for the two components of the forces σ and ξ. Coordinates y and z are fixed.

FIG. 21. Fourier transform of the space cross correlation between the force σ and the force ξ. Coordinates y and z are fixed.

tice that the cross correlations are one order of magnitude weaker than the direct correlations. The cross correlations involving ξ_{12} are essentially zero, while the correlations involving ξ_{11} display a first overall decay up to $k=k_c$, followed by an extra bump up to the end of the inertial range ($k=40$). In Sec. III D, we will show that this feature is actually related to the energy cascade.

One may also note that the two noises are spatially very intermittent. In Fig. 22, we show isosurfaces of the modulus of the noises, corresponding to 3.5 times the rms value. For comparison, the same plot is made for the vorticity. One observes well-defined patches of σ which are strongly correlated with areas of strong vorticity. In the case of ξ, the patches are much more space filling. The longitudinal component ξ_{11} is characterized by smaller-scale structures than the transverse component ξ_{12}.

To obtain an indication about the scale variation of the statistical properties of the noises, we also computed the PDFs of the noise spatial increments $\delta\sigma_{i\ell}=\sigma(x+\ell)-\sigma(x)$ and $\delta\xi_{ij\ell}=\xi_{ij}(x+\ell)-\xi_{ij}(x)$. Note that the first of these quantities is directly related to the Gabor transform of
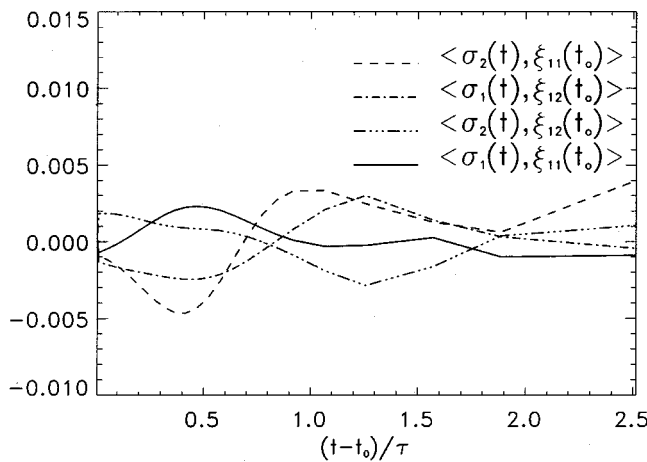

FIG. 20. The cross correlation in time between the forces σ and ξ ($\tau=0.19$).
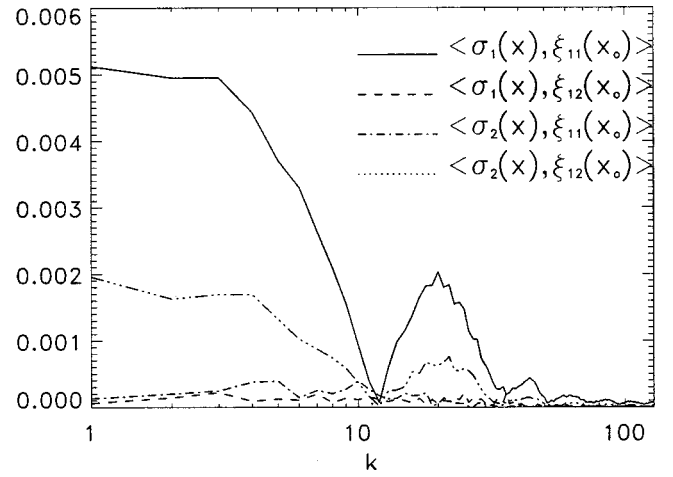
the additive noise, whereas the second one contains some useful information about the time correlations via the Taylor hypothesis (which is valid locally because the large-scale velocity is typically greater than the small-scale one). Figure 23 shows the results of the longitudinal and transverse increments for the first component of the additive noise σ_1 and the equivalent results for the component ξ_{11} of the multiplicative noise are shown in Fig. 24. The PDFs are displayed for $\ell=2\pi/256$ and $2\pi/4$. One observes wide, quasialgebraic tails for the additive noise, similar to those observed for the PDFs of the velocity derivatives. The PDFs of ξ_{11} are much closer to Gaussian statistic.

C. The turbulent viscosity

In Sec. II C, we discussed the influence of two prescriptions for the turbulent viscosity, one based on the RNG, one taken simply as constant. In the sequel, we shall use the simple formula:

$$\nu_t = \left(\nu_0^2 + B^2 \left(\frac{u}{k} \right)^2 \right)^{1/2},$$ (24)

where ν_0 and B are constants and $u=k^d \, \mathrm{Im} \, \hat{u}$ is the velocity increment over a distance $1/k$ (hereafter we drop δ in δu). When $B=0$, this formula provides the constant turbulent viscosity. When $\nu_0=0$, it provides a dimensional analog of the RNG viscosity, and tends to zero as k tends to infinity.

D. Statistical properties of the velocity increments

We are now going to derive qualitative results by adopting two complementary points of view: In the first one, we will study the statistical properties of the velocity increments in the frame of reference moving together with the wave packets in (k, x) space. This corresponds to a Lagrangian description in the scale space. In the second approach, we replace time with its expression in terms of k, as it would follow from the ray equation (22). This will give as an equation at a fixed k which corresponds to an Eulerian description. As a further simplification, we shall leave for further study the possible correlation between longitudinal and
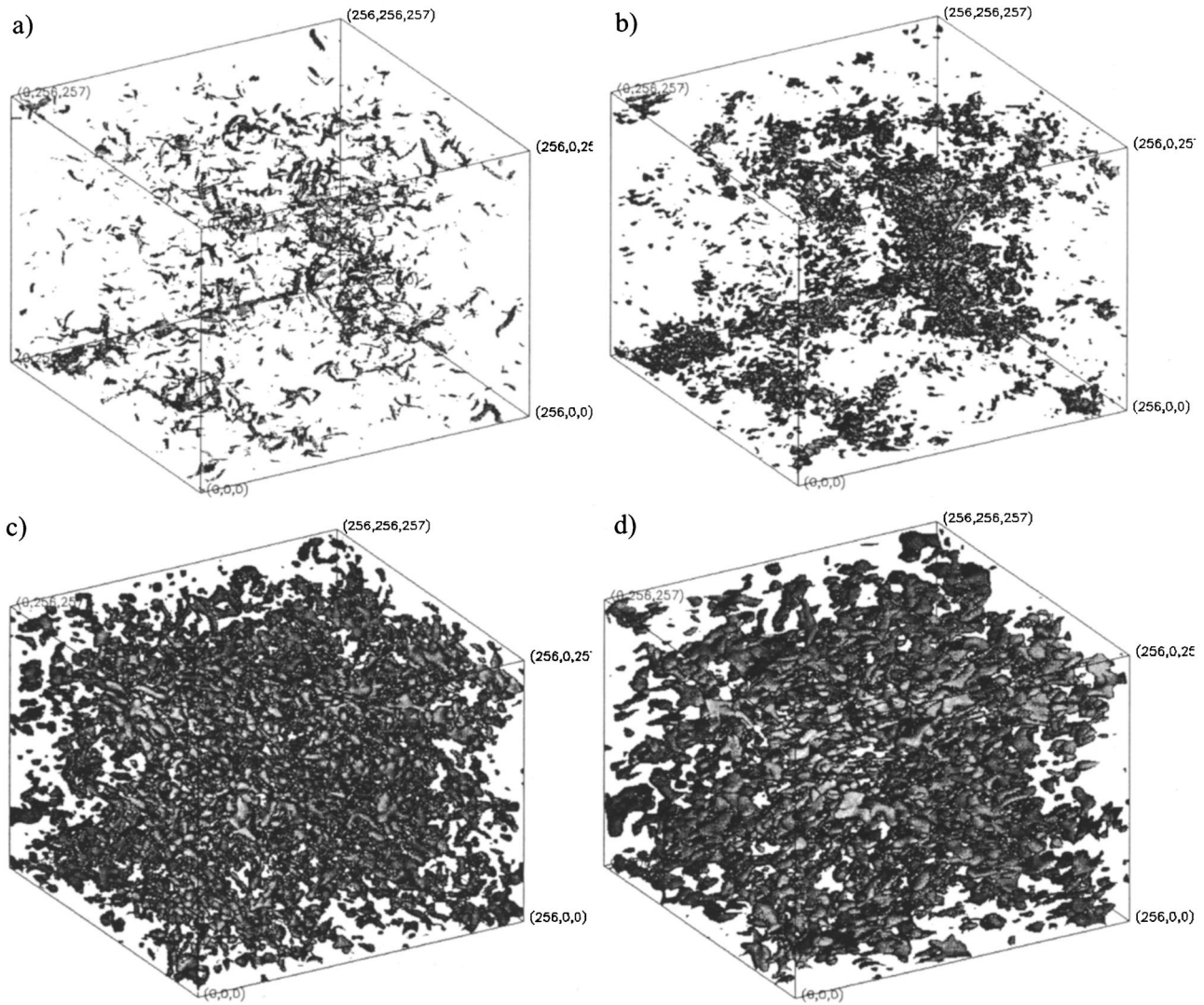
FIG. 22. Isovalue (3.5 times the rms) at $t_0=0$ of (a) the absolute value of vorticity, (b) the corresponding additive force ($|\sigma|$), (c) $\xi_{11}=\partial U_x/\partial x$, and (d) $\xi_{12}=\partial U_x/\partial y$.

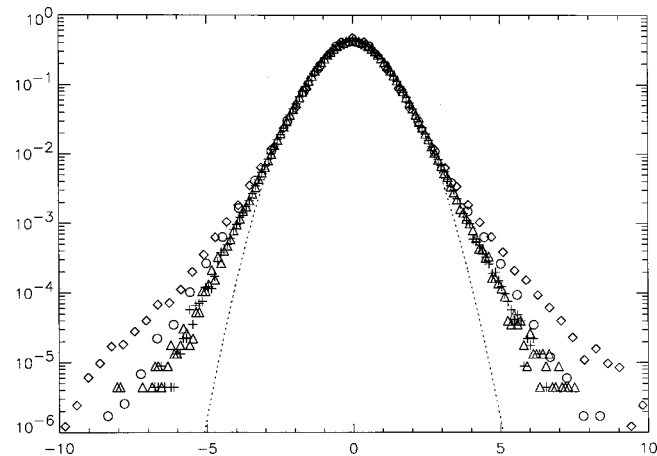FIG. 23. PDFs of the increments $\sigma_1(x+\ell_1,y,z)-\sigma_1(x,y,z)$ for ℓ_1 $=2\pi/256$ (circles) and $\ell_1=2\pi/4$ (crosses) and $\sigma_1(x,y+\ell_2,z)$ $-\sigma_1(x,y,z)$ for $\ell_2=2\pi/256$ (triangles) and $\ell_2=2\pi/4$ (diamonds) (the dotted line corresponds to Gaussian statistics).
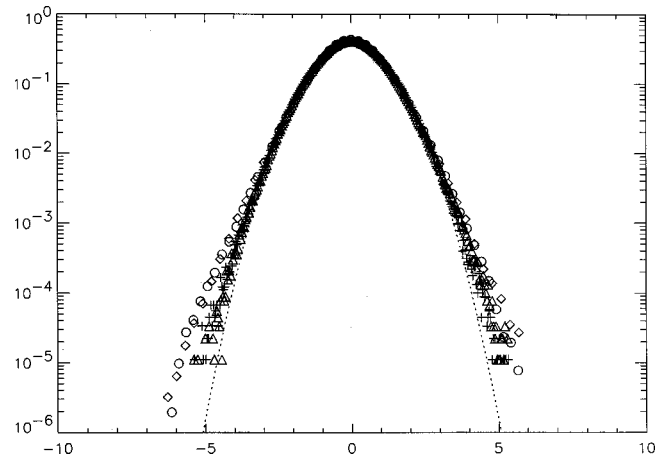
FIG. 24. PDFs of the increments $\xi_{11}(x+\ell_1,y,z)-\xi_{11}(x,y,z)$ for ℓ_1 $=2\pi/256$ (circles) and $\ell_1=2\pi/4$ (crosses) and $\xi_{11}(x,y+\ell_2,z)$ $-\xi_{11}(x,y,z)$ for $\ell_2=2\pi/256$ (triangles) and $\ell_2=2\pi/4$ (diamonds) (the dotted line corresponds to Gaussian statistics).

Phys. Fluids, Vol. 13, No. 7, July 2001

Nonlocality and intermittency in 3-D turbulence   2007

transverse velocity increments described for example in Ref. 41 and consider a one-dimensional version of (19), treating the quantity $u = k \, \text{Im} \, \hat{u}$ as a ''velocity increment'' over the distance $l = 2\pi/k$,

$$D_t u = u\xi + \sigma_\perp - \nu_t k^2 u, \tag{25}$$

$$\dot{k} = -k\xi. \tag{26}$$

Here, we assumed the forcing to be symmetric such that it does not produce any $\text{Re} \, \hat{u}$. This model can also be viewed as a passive scalar in a compressible one-dimensional flow. Artificial introduction of compressibility is aimed at modeling the RDT stretching effect which appears only in the higher number of dimensions for incompressible fluids.

Study of the noises in Sec. III B revealed their rich and complex behavior. As a first simplifying step, we disregard these complexities and use the Gaussian, delta correlated approximation, as will be done in Secs. III D 1 and III D 2. Given a rather short time correlation of σ, our delta approximation is rather safe. The delta approximation for ξ is more debatable, and the performance of such a model should be further examined in future. Also, the Gaussian hypothesis is obviously only valid at large scale, and for ξ_{11}. Therefore, the generalization of our results for non-Gaussian noises would be very interesting, and is the subject of ongoing research. In the sequel, we consider the functions α, D, and λ as free parameters.

1. The Lagrangian description

In the frame of reference moving with the wave packets in (k, x) space, the left-hand side of (25) becomes simply the time derivative. On the other hand, k has to be replaced in terms of its initial value k_0 and time everywhere including the noises σ and ξ. Such a transformation from the laboratory to the moving frame can obviously change the statistics of σ and ξ. In the Lagrangian description we will assume that we deal with noises which are Gaussian in the moving frame with correlations functions

$$\langle \sigma_\perp(k(t),t)\sigma_\perp(k'(t),t')\rangle = 2\alpha\delta(t-t'),$$

$$\langle \xi(k(t),t)\xi(k'(t),t')\rangle = 2D\delta(t-t'), \tag{27}$$

$$\langle \xi(k(t),t)\sigma_\perp(k'(t),t')\rangle = 2\lambda\delta(t-t'),$$

where coefficients α, D, and λ depend on the scale via k_0. With these noise, (25) becomes a Langevin equation for the velocity increments, where ξ is a multiplicative noise, $\sigma_\perp$ is an additive noise, and $\nu_t k^2 u$ the (nonlinear) friction. The multiplicative noise is produced by the interaction of two small scales with one large scale whereas the additive noise is due to a merger of two large scales into one small scale (therefore, the latter acts at the largest among the small scales). For Gaussian, delta correlated noises, this Langevin equation leads to a Fokker–Planck equation for the probability distribution $P_k(u,t)$ of the velocity increment u,

$$\partial_t P_k = \partial_u(\nu_t k^2 u P_k) + D_k \partial_u(u\partial_u u P_k) - \lambda_k \partial_u(u\partial_u u P_k)$$

$$- \lambda_k \partial_u^2(u P_k) + \alpha_k \partial_u^2 P_k, \tag{28}$$

where we have taken into account the fact that, due to homogeneity, ξ and σ have a zero mean. Here, we dropped the subscript 0 in k_0 and the dependence of all involved quantities on the scale is simply marked by the subscript k (the scale dependence α, D, and λ is still unspecified). The stationary solution of (28) is

$$P_k(u) = C_k \exp \int_0^u \frac{-\nu_t k^2 y - Dy + \lambda}{Dy^2 - 2\lambda y + \alpha} \, dy, \tag{29}$$

where C_k is a normalization constant. The integral appearing in (29) can be explicitly computed in two regimes: In the first one, for $u \ll k\nu_0$, we have ($\nu_t = \nu_0$), and we simply get

$$P_k(u) = \frac{C}{(Du^2 - 2\lambda u + \alpha)^{1/2 + \nu_0 k^2/(2D)}}. \tag{30}$$

The range of u for which the PDF follows this algebraic law decreases with increasing scales. It is the largest (and hence it is best observed) at the dissipative scale, where the velocity increments are equivalent to velocity derivative or to vorticity. Several remarks are in order about this expression. First, notice that the distribution is regularized around $u = 0$ by the presence of the parameter α, but then displays algebraic tails. These are well-known features of random multiplicative process with additive noise (see, e.g., Ref. 42). The occurrence of algebraic tails in vorticity PDFs has been noted before in Refs. 43 and 44 in the context of 2-D turbulence. However, processes with algebraic tails are characterized by divergent moments. These divergences can be removed by taking into account finite size effects, like physical upper bounds on the value of the process (see, e.g., Ref. 14 for discussion and references) which introduce a cutoff in the probability distribution. This effect is automatically taken into account in our simple model, via the turbulent viscosity, which prevents unbounded growth of velocity fluctuations and introduces an exponential cutoff.

Indeed, in the regime $u \gg k\nu_0$, we see that

$$\frac{d \ln P}{du} \approx \frac{-u|u|}{Du^2 - 2\lambda u + \alpha}. \tag{31}$$

This means that at large u the PDF decays like an exponential, or even faster if $D = 0$ (see the following). The exponential cutoff has been observed in high Reynolds number turbulence.[45] In 2-D turbulence, this feature has also been noted by Min et al.,[44] and here finds a detailed explanation.

Another important observation is that the PDFs have an intrinsic skewness, which can be traced back to the nonzero value of λ, i.e., to the correlation between the multiplicative and the additive noise. The physical picture associated with this correlation is related to the correlation between vorticity (present in the large scale strain tensor) and stretching (associated with the term $U\nabla U$, present in σ), which is the motor of the energy cascade.[41] The importance of the additive noise in the skewness generation has been stressed before.[46] We find here its detailed explanation. Note also that the trends toward Gaussian large scale behavior of the velocity increments can be easily accounted for if the multiplicative noise tends to zero at large scale ($D, \lambda \to 0$). In such case, the process becomes purely additive, and the limiting PDF is
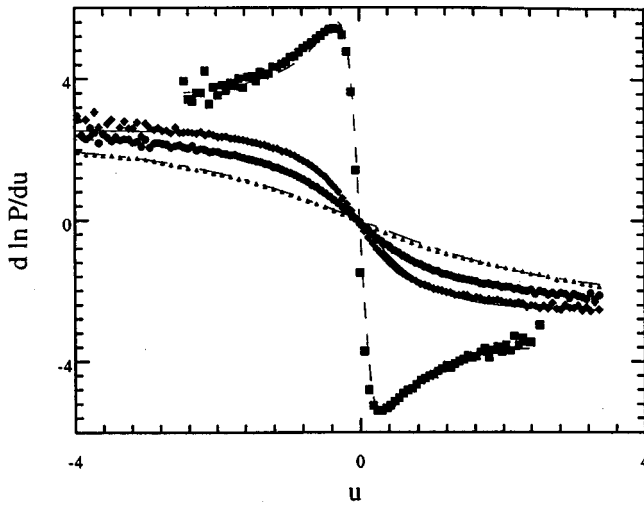
FIG. 25. Fit of $d \ln P/du$ for the transverse increments, at $1/k=2$ (squares), $1/k=32$ (diamonds), $1/k=42$ (circles), and $1/k=52$ (triangles). The fits via formula (32) are given by lines. Note the good quality of the fit. Similar fits for other scale separations and in the longitudinal case were obtained.
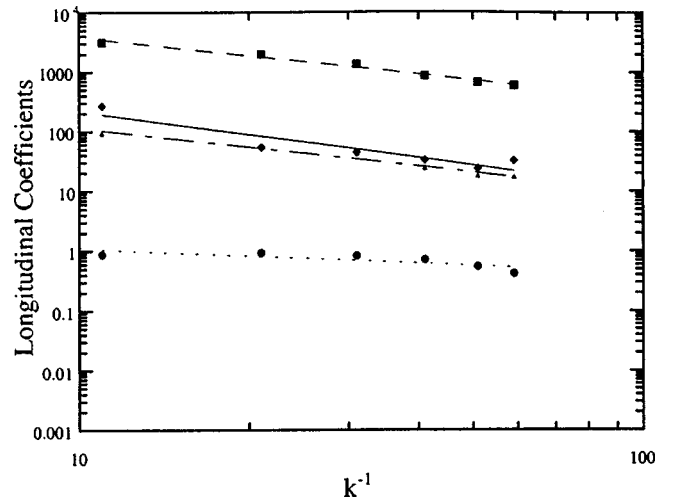

FIG. 26. Coefficient of the fit of $d \ln(P)/du$ with (32) as a function of $1/k$ for longitudinal velocity increments: m_1 (squares), m_2 (open diamonds), m_3 (circles), and m_4 (closed diamonds). The lines are the power-law fits: $k^{-0.79}$ (long-dashed line); $k^{-1.52}$ (short-dashed line); $k^{-0.36}$ (dotted line), and $k^{-1.2}$ (dash-dot line).

Gaussian for u independent turbulent viscosity, or can also fall faster than a Gaussian [like $\exp(-u^3)$, for $\nu_t \propto u$]. Such a supra Gaussian behavior has been noted before.[41] In between the dissipative and the largest scale, the transition operates via PDFs looking like stretched exponential.

This qualitative feature can be tested by comparison with the numerical PDFs. Our model predicts that $d \ln P/du$ should behave like the ratio

$$\frac{d \ln P}{du} = \frac{-u\sqrt{(m_1 u)^2 + m_2^2} - m_4 u + m_3}{m_4 u^2 - 2m_3 u + m_5}. \tag{32}$$

Without loss of generality, we can factorize out the parameter m_5. The fit therefore only contains four free parameters, which can be easily related to the physical parameters of the problem. We have computed this derivative for the PDF of longitudinal and transverse velocity increments at various scales, and performed the four parameters fit. Examples are shown in Fig. 25. Observe the good quality of the fit, but we stress that there is a rather large uncertainty in the determination of the parameter of the fits, which sometimes cannot be determined better than up to a factor of 2 by our fit procedure (a standard least-squares fit). The scale dependence of the coefficients of the fit is shown in Figs. 26 and 27. Note that since transverse velocity increments are symmetrical by construction, we have set $m_3 = 0$ in the fit. Note that in the longitudinal case, m_3 is smaller than the other coefficients by two orders of magnitude. This features the smallness of the skewness, and the weakness of the correlation between the multiplicative and the longitudinal noise (see Sec. III B). The parameters have a rough power law behavior (see Figs. 26 and 27). Theoretically, one expects the ratio m_1/m_2 to behave like $1/(\nu_0 k)$, if (24) holds. The power-law fits of Figs. 26 and 27 provide a dependence of $k^{0.53}$ for the longitudinal case, and $k^{-0.54}$ for the transverse case, corresponding to a scale dependence of ν_0 given by $k^{1.53}$ and $k^{0.46}$.

2. The Eulerian description

We now consider (25), again in the moving with the wave packet frame, but now we change the independent variable from t to $k=k(t)$ which satisfies (26). We get

$$\frac{du}{d \ln k} = -\mathcal{P}u + \frac{\nu_t k^2}{\xi} - \frac{\sigma_\perp}{\xi}, \tag{33}$$

where $\mathcal{P}$ is a number accounting for the projection operator over scales smaller than the cutoff $1/k_c$. This is a way to mimic higher-dimensional effects in our one-dimensional model. Equation (33) is again a Langevin equation for velocity increments in the scale space, with multiplicative and additive noises which are now expressed in an Eulerian
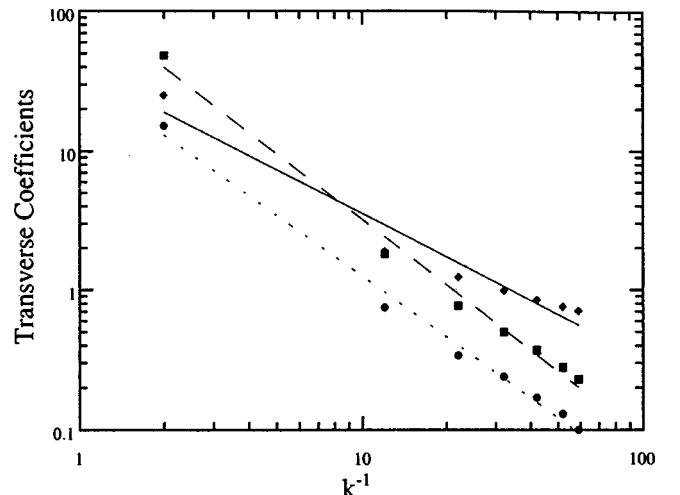

FIG. 27. Coefficient of the fit of $d \ln(P)/du$ with (32) as a function of $1/k$ for transverse velocity increments: m_1 (squares), m_2 (diamonds), and m_4 (circles). The lines are the power-law fits: $k^{-1.56}$ (long-dashed line); $k^{-1.04}$ (line); and $k^{-1.45}$ (dotted line).

Phys. Fluids, Vol. 13, No. 7, July 2001

Nonlocality and intermittency in 3-D turbulence   2009

form. Similar Langevin processes have been proposed before to explain the scale dependence of velocity increments[47,48,40] but without additive noise.[49]

The noises in this Langevin equation are different from the noises appearing in the Lagrangian representation and they would have a complicated statistics if we assumed that σ and ξ were Gaussian in the Lagrangian representation. However, we can simply assume here that the noises are Gaussian and delta correlated in the Eulerian representation (which is different from the assumption of the previous section) and redefine α, D, and λ as

$$\langle \sigma_\perp(k,t(k))\xi^{-1}(k,t(k))\sigma_\perp(k',t(k'))\xi^{-1}(k',t(k'))\rangle$$
$$= 2\alpha\delta(k-k'),$$

$$\langle \xi^{-1}(k,t(k))\xi^{-1}(k',t(k'))\rangle = 2D\delta(k-k'), \quad (34)$$

$$\langle \xi^{-1}(k,t(k))\sigma_\perp(k',t(k'))\xi^{-1}(k',t(k'))\rangle = 2\lambda\delta(k-k').$$

This allows one to derive the Fokker–Planck equation corresponding to (33),

$$k\partial_k P(u,k) = \partial_u(\mathcal{P}uP) + D\partial_u(\nu_t k^2 u\partial_u[\nu_t k^2 uP])$$
$$- \lambda\partial_u(\nu_t k^2 u\partial_u P) - \lambda\partial_u^2(\nu_t k^2 uP) + \alpha\partial_u^2 P.$$
$$(35)$$

We may use (35) to derive an equation for the moments, by multiplication by u^n and integration over u. With the shape of the turbulent viscosity given by (24), we get

$$k\partial_k\langle u^n\rangle = -\zeta(n)\langle u^n\rangle + nDB^2k^2\langle u^{n+2}\rangle$$
$$- \lambda n(2n-1)\nu^2 k^2\left\langle\frac{u^{n-1}}{\nu_t}\right\rangle$$
$$- 2n^2\lambda B^2\left\langle\frac{u^{n+1}}{\nu_t}\right\rangle + \alpha n(n-1)\langle u^{n-2}\rangle, \quad (36)$$

where $\zeta(n) = n\mathcal{P} - n^2 Dk^4\nu^2$ is the zero-mode scaling exponent. For $n=1$ and taking into account the constraints that $\langle u\rangle = 0$ (homogeneity), one gets a sort of generalized Karman–Horwath equation:

$$\langle u^3\rangle = \frac{\lambda\nu^2}{DB^2}\left\langle\frac{1}{\nu_t}\right\rangle + \frac{2\lambda}{Dk^2}\left\langle\frac{u^2}{\nu_t}\right\rangle. \quad (37)$$

As in the Lagrangian case, this means that skewness (related to nonzero $\langle u^3\rangle$) is generated through nonzero values of λ, i.e., through correlations of the multiplicative and the additive noises. However, due to the turbulent viscosity, we cannot explicitly solve the hierarchy of equation. In many homogeneous turbulent flows, however, the skewness (proportional to λ) is quite small, and moments of order $2n+1$ are generally negligible in front of moments of order $2n+2$. For *even* moments, this remark suggests that to first order in the skewness, and for $2n>1$, the dynamics is simply given by

$$k\partial_k\langle u^{2n}\rangle = -\zeta(2n)\langle u^{2n}\rangle + 2nDB^2k^2\langle u^{2n+2}\rangle$$
$$+ \alpha 2n(2n-1)\langle u^{2n-2}\rangle + O(\lambda^2). \quad (38)$$

Note that D/α is given by the parameter m_4 in our fit, and is such that Dk^2/α increases with k (see Figs. 26 and 27). Therefore, at small scales, the dominant balance is

$$k\partial_k\langle u^{2n}\rangle = 2nDB^2k^2\langle u^{2n+2}\rangle. \quad (39)$$

The solution is $\langle u^{2n}\rangle \propto k^{-2n}$. This is the usual ''regular'' scaling in the dissipative zone. For larger scales, $DB^2k^2 \ll \alpha$, and if α varies like a power law, the general solution of (38) is a sum of power laws:

$$\langle u^{2n}\rangle = \sum_{p=0}^{n} a_p\alpha^{n-p}k^{-\zeta(2p)}. \quad (40)$$

This solution illustrates the famous mechanism of ''zero-mode intermittency.''[9] Here, the zero mode is the solution of the homogeneous part of Eq. (38), i.e., a power law of exponent $-\zeta(2n)$. Without the zeroth mode, responsible for the first $n-1$ scaling laws, the $2n$th moment will scale in general like $\alpha(k)^n$ (provided one assumes that this dominates the other term), i.e., will be related to the turbulent forcing. This is the standard Kolmogorov picture. When the zeroth mode is taken into account, the moment now includes new power laws, whose exponent is independent of the external forcing, and which can be dominant in the inertial range, thereby causing anomalous scaling. In the present case, the scaling exponent is quadratic in n, and reflects the log-normal statistics induced by the Gaussian multiplicative noise, in agreement with the latest wavelet analysis of Arneodo *et al.*[50] Note also that the competition between the zeroth-mode scaling and the scaling due to external forcing forbids the moments to scale like a power law, thereby generating a breaking of the scale symmetry.

For *odd* moments, we cannot perform any rigorous expansion because all the terms of the equation are of order λ. For low order moments, however, the computation of $\langle u^{n+1}/\nu_t\rangle$ mainly involves velocity increments close to the center of the distribution, for which $\nu_t \approx \nu_0$. So, for low order, it is tempting to approximate the equation for the odd-order moments by

$$k\partial_k\langle u^{2n+1}\rangle \approx -\zeta(2n+1)\langle u^{2n+1}\rangle$$
$$- 2n^2\lambda B^2\langle u^{2n+2}\rangle\nu^{-1}. \quad (41)$$

This approximation is only valid in the inertial range, where the last term of (36) can be neglected. An immediate consequence of this loose approximation is that $\zeta(2n+1) = \zeta(2n+2)$ in the inertial range. Odd moments (without absolute values) are very difficult to measure because of cancellation effects which introduce a lot of noise. In our case, due to our limited inertial range, we cannot compute these exponents with a sufficient degree of accuracy. A careful investigation performed in a high Reynolds number boundary layer[30] however seems to be in agreement with our prediction, as is shown in Fig. 28: It is striking to observe that $\zeta(5) \approx \zeta(6)$, $\zeta(7) \approx \zeta(8)$, etc., making the curve look as if odd and even scaling exponents are organized on a separate curve.[51] A second independent experimental check of our prediction (41) is that $(\zeta(2n+2) - \zeta(2n+1))\langle u^{2n+1}\rangle/\langle u^{2n+2}\rangle$ should scale, for $n>3$ like n^2. Figure 29 shows that this is indeed the case.
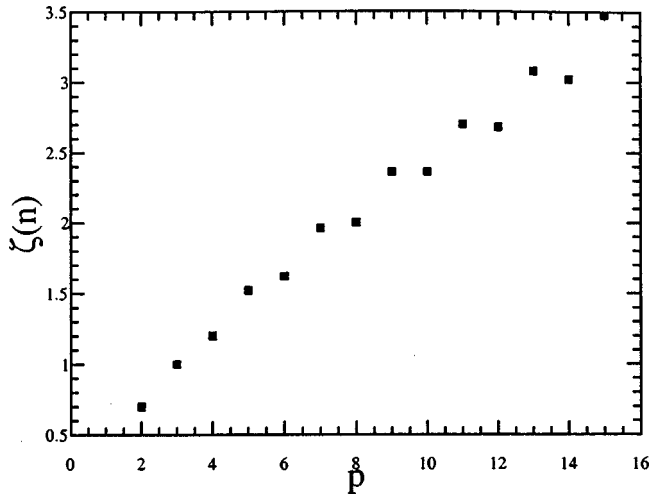
FIG. 28. Exponents of the structure function in a high Reynolds number boundary layer (Ref. 28). Note the tendency for $\zeta(2n+1)=\zeta(2n+2)$ for $n>3$.

IV. DISCUSSION

In this paper, we have shown that nonlocal interactions are responsible for intermittency corrections in the statistical behavior of 3-D turbulence. Removal of the local interaction in numerical simulations leads to a substantial increase in the number of the tornado-like intense vortex filaments and to stronger anomalous corrections in the higher cumulants of the velocity increments. It is also accompanied by a modification of the energy transfer in the inertial range, tending to create a flatter energy spectrum. The intermittency corrections and the spectra are close to that observed in high Reynolds number boundary layer, suggesting that the nonlocal interactions prevail in this geometry. This could be explained by the presence of the mean flow, which geometrically favors nonlocal triads in the Fourier transform of the nonlinear interactions. We showed that replacing the removed local interactions by a simple turbulent viscosity term allows one
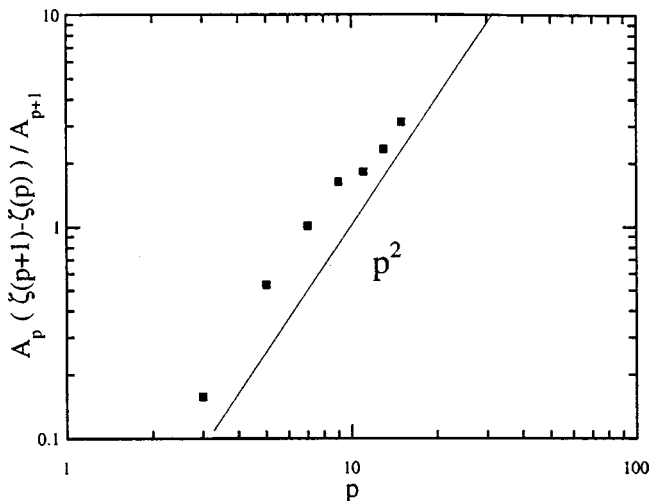

FIG. 29. $(\zeta(2n+2)-\zeta(2n+1))A_{2n+1}/A_{2n+2}$ as a function of n in a high Reynolds number boundary layer. Here A_n is the prefactor of the (nondimensional) structure function of order n. The line is n^2, the prediction of our model.

to restore the correct intermittency and the energy characteristics. Our results agree with the belief that intermittency is related to thin vortices amplified by the external large scale strain similar to the classical Burgers vortex solution. Local interactions can be viewed at mutual interaction of these thin intense vortices which result in their destruction, which is also in agreement with our results.

To prove that the enhanced intermittency is not simply the result of the stronger small-scale observed in the RDT simulation, we performed yet another numerical experiment in which the nonlocal interactions were neglected and only the local ones retained. This resulted in an even higher (than in RDT) level of the small scales but it exhibited much less intermittency, which confirms our view that nonlocality is crucial for generation of the intermittent structures.

The result that the net effect of the local interactions is to destroy the intermittent structures is at odds with a very common belief that the intermittency is due to the vortex reconnection process which takes a form of a finite time vorticity blow-up. Indeed, the latter is a strongly nonlinear process in which the local vortex–vortex interactions are important. However, this process seems to be dominated by another local processes the net result of which is to destroy the high-vorticity structures rather than to create them. It would be premature to claim, however, that the same is true at any arbitrarily high Reynolds number.

Our numerical approach sets severe limitations to the value of the Reynolds number we are able to explore. In this context, it is interesting to point out that preliminary tests regarding the importance of nonlocal interactions have been conducted on a velocity field coming from a very large Reynolds number boundary layer.[52] Even though the test is not complete (the probes only permit the accurate measurement of special components of the velocity field), it tends to suggest that nonlocal interactions dominate the local interactions by several orders of magnitude. Our results would also explain the findings of the Lyon team,[53] who found that when probing fluid area closer and closer to a large external vortices, or to a wall boundary, one could measure energy spectra moving from a $k^{-5/3}$ law toward a k^{-1} spectra, while anomalous corrections in scaling exponents would become more pronounced. In light of our study, this could be simply explained by a trend toward more nonlocal dynamics via the mean-shear effects at the wall.

Based on the conclusions of our numerical study, we developed a new model of turbulence to study the intermittency. It has the form of a Langevin equation for the velocity increments with coupled multiplicative and additive noise. We showed how this model could be used to understand qualitatively certain observed features of intermittency and anomalous scaling laws. Among other things, we showed how the coupling between the two forces is related to the skewness of the distribution, and how algebraic and stretched exponential naturally arise from the competition between the multiplicative and the additive noise. We tested our qualitative predictions with experimental and numerical data, and found good general agreement. To be able to turn our model into a tool for ''quantitative'' study of the intermittency, several developments are needed. The first one is to consider the

multidimensional version of our model to be able to couple longitudinal and transverse increments. The scale dependence of the turbulent viscosity and of the forcing needs to be further investigated, possibly using tools borrowed from the renormalization group theory (see, e.g., Ref. 26). Also, the non-Gaussianity of the noises could be taken into account.

In 1994, Kraichnan[54] proposed an analytically solvable, new model for the passive scalar, which provided a substantial increase of our understanding of the passive scalar intermittency. Our model, built using the nonlocal hypothesis, is a direct heir of this philosophy in that, as in passive scalars, all important intermittency effects are produced via a linear dynamics. The nonlinear (local) scale interactions are important too because they are the main carrier of the energy cascade, but it is only their mean effect and not statistical details that are essential.

ACKNOWLEDGMENTS

[1] E. D. Siggia, ''Numerical study of small-scale intermittency in 3-dimensional turbulence,'' J. Fluid Mech. **107**, 375 (1981).

[2] A. Vincent and M. Meneguzzi, ''The spatial structure and statistical properties of homogenous turbulence,'' J. Fluid Mech. **225**, 1 (1991).

[3] Z. S. She, E. Jakson, and S. A. Orszag, ''Intermittent vortex structures in homogeneous isotropic turbulence,'' Nature (London) **344**, 226 (1990).

[4] A. N. Kolmogorov, ''The local structure of turbulence in incompressible viscous fluid for very large Reynolds number,'' C. R. Acad. Sci. URSS **30**, 301 (1941).

[5] A. N. Kolmogorov, ''A refinement of previous hypotheses concerning the local structure of turbulence in a viscous incompressible fluid at high Reynolds number,'' J. Fluid Mech. **13**, 82 (1962).

[6] G. Parisi and U. Frisch, ''On the singularity structure of fully developed turbulence,'' in *Turbulence and Predictability in Geophysical Fluid Dynamics*, edited by M. Ghil, R. Benzi, and G. Parisi, Proceedings of the International School of Physic ''E. Fermi,'' Varenna, Italy, 1983 (North-Holland, Amsterdam, 1985).

[7] U. Frisch, *Turbulence: The Legacy of A. N. Kolmogorov* (Cambridge University Press, Cambridge, 1995).

[8] B. Castaing, ''Consequences of an extremum principle in turbulence,'' J. Phys. (France) **50**, 147 (1989).

[9] K. Gawedski and A. Kupiainen, ''Anomalous scaling of passive scalar,'' Phys. Rev. Lett. **75**, 3834 (1995).

[10] B. Dubrulle, ''Finite size scale invariance,'' Eur. Phys. J. B **14**, 757 (2000).

[11] J. G. Brasseur and C. H. Wei, ''Interscale dynamics and local isotropy in high Reynolds number turbulence within triadic interactions,'' Phys. Fluids **6**, 842 (1994).

[12] J. A. Domaradzki, W. Liu, C. Härtel, and L. Kleiser, ''Energy transfer in numerically simulated wall-bounded turbulent flows,'' Phys. Fluids **6**, 1583 (1994).

[13] J.-P. Laval, B. Dubrulle, and S. Nazarenko, ''Nonlocality of interaction of scales in the dynamics of 2D incompressible fluids,'' Phys. Rev. Lett. **83**, 4061 (1999).

[14] J.-P. Laval, B. Dubrulle, and S. Nazarenko, ''Dynamical modeling of sub-grid scales in 2D turbulence,'' Physica D **142**, 231 (2000).

[15] V. Borue, ''Spectral exponents of entrophy cascade in stationary homoge-

[16] neous two dimensional turbulence,'' Phys. Rev. Lett. **71**, 3967 (1994).

[16] A. Arneodo, C. Baudet, F. Belin, R. Benzi, B. Castain, B. Chabaud, R. Chavarria, S. Ciliberto, R. Camussi, and F. Chilla, ''Structure functions in turbulence in various flow configuration at Reynolds number between 30 and 5000 using extended self-similarity,'' Europhys. Lett. **34**, 411 (1996).

[17] A. A. Townsend, *The Structure of Turbulent Shear Flow*, 2nd ed. (Cambridge University Press, Cambridge, 1976).

[18] J.-P. Laval and B. Dubrulle, ''Numerical validation of a dynamical turbulent model of turbulence,'' Phys. Rev. Lett. (submitted).

[19] S. Nazarenko and J.-P. Laval, ''Non-local 2D turbulence and Batchelor's regime for passive scalars,'' J. Fluid Mech. **408**, 301 (2000).

[20] A. E. Perry, S. Henbest, and M. S. Chong, ''A theoretical and experimental study of wall turbulence,'' J. Fluid Mech. **165**, 163 (1986).

[21] S. Nazarenko, ''Exact solutions for near-wall turbulence theory,'' Phys. Lett. A **264**, 444 (2000).

[22] A. Vincent and M. Meneguzzi, ''The dynamics of vorticity tubes in homogeneous turbulence,'' J. Fluid Mech. **258**, 245 (1994).

[23] R. H. Kraichnan, ''Eddy viscosity in two and three-dimensions,'' J. Atmos. Sci. **33**, 1521 (1976).

[24] B. Dubrulle and U. Frisch, ''Eddy viscosity of parity-invariant flow,'' Phys. Rev. A **43**, 5355 (1991).

[25] V. Yakhot and S. A. Orzag, ''Renormalisation group analysis of turbulence. I. Basic theory,'' J. Sci. Comput. **1**, 3 (1986).

[26] V. M. Canuto and Dubovikov, ''A dynamical model for turbulence. I. General formalism,'' Phys. Fluids **8**, 571 (1996).

[27] R. Benzi, S. Ciliberto, R. Tripiccione, F. Baudet, F. Massaioli, and S. Succi, ''Extended self similarity in turbulent flows,'' Phys. Rev. E **48**, R29 (1993).

[28] B. Dhruva, Y. Tsuji, and K. R. Sreenivasan, ''Transverse structure functions in high-Reynolds-number turbulence,'' Phys. Rev. E **56**, R4928 (1997).

[29] R. Camussi and R. Benzi, ''Hierarchy of transverse structure functions,'' Phys. Fluids **9**, 257 (1997).

[30] G. Stolovidsky, K. R. Sreenivasan, and A. Juneja, ''Scaling functions and scaling exponents in turbulence,'' Phys. Rev. E **48**, R3217 (1993).

[31] F. Toschi, G. Amati, S. Succi, and R. Piva, ''Intermittency and structure functions in channel flow turbulence,'' Phys. Rev. Lett. **82**, 5044 (1999).

[32] E. B. Gledzer, ''System of hydrodynamic type admitting two quadratic integrals of motions,'' Sov. Phys. Dokl. **18**, 216 (1973).

[33] M. Yamada and K. Ohkitani, ''Lyapunov spectrum of a model of two-dimensional turbulence,'' Phys. Rev. Lett. **60**, 983 (1988).

[34] M. Yamada and K. Ohkitani, ''Temporal intermittency in the energy cascade process and local Lyapunov analysis in fully-developed turbulence,'' Prog. Theor. Phys. **81**, 329 (1989).

[35] Th. Dombre (private communication).

[36] S. Nazarenko, N. K.-R. Kevlahan, and B. Dubrulle, ''WKB theory for rapid distortion of inhomogeneous turbulence,'' J. Fluid Mech. **390**, 325 (1999).

[37] S. Nazarenko, N. K.-R. Kevlahan, and B. Dubrulle, ''Nonlinear RDT theory of near-wall turbulence,'' Physica D **139**, 158 (2000).

[38] A. Tsinober, E. Kit, and T. Dracos, ''Experimental investigation of the field of velocity gradients in turbulent flows,'' J. Fluid Mech. **82**, 169 (1992).

[39] B. Andreotti, ''Studying Burger's model to investigate the physical meaning of the alignments statistically observed in turbulence,'' Phys. Fluids **9**, 735 (1997).

[40] P. Marcq and A. Naert, ''A Langevin equation for turbulent velocity increments,'' Phys. Fluids (to be published).

[41] B. Andreotti, ''Action et réaction entre étirement et rotation, du laminaire au turbulent,'' Ph.D. thesis, Université de Paris 7, 1997.

[42] H. Nakao, ''Asymptotic power law of moments in a random multiplicative process with weak additive noise,'' Phys. Rev. E **58**, 1591 (1998).

[43] J. Jimenez, ''Algebraic probability density tails in decaying isotropic two-dimensional turbulence,'' J. Fluid Mech. **313**, 223 (1996).

[44] I. A. Min, I. Mezic, and A. Leonard, ''Lévy stable distribution for velocity and velocity difference in systems of vortex elements,'' Phys. Fluids **8**, 1169 (1996).

[45] A. Praskovsky and S. Oncley, ''Probability density distribution of velocity differences at very high Reynolds numbers,'' Phys. Rev. Lett. **73**, 3399 (1994).

[46] B. Dubrulle, ''Affine turbulence,'' Eur. Phys. J. B **13**, 1 (2000).

[47] R. Friedrich and J. Peinke, ''Description of a turbulent cascade by a Fokker–Planck equation,'' Phys. Rev. Lett. **78**, 863 (1997).

[48] Ph. Marcq and A. Naert, ''A Langevin equation for the energy cascade in

fully-developed turbulence,'' Physica D **124**, 368 (1998).

[49] At a turbulence in Dresden, in August 1998, R. Friedrich however suggested the possibility of two interacting multiplicative and additive noises in his presentation.

[50] A. Arneodo, S. Maneville, J. F. Muzy, and S. G. Roux, ''Revealing a lognormal cascading process in turbulent velocity statistics with wavelet analysis,'' Philos. Trans. R. Soc. London, Ser. A **357**, 2415 (1999).

[51] L. Zubair, ''Studies in turbulence using wavelet transform for data compression and scale separation,'' Ph.D. thesis, Yale University, 1993.

[52] J. Carlier, J.-P. Laval, J. M. Foucaut, and M. Stanislas, ''Non-locality of the interaction of scales in high Reynolds number turbulent boundary layer,'' C. R. Acad. Sci., Ser. IIb: Mec., Phys., Chim., Astron. **329**, 1 (2001).

[53] J. F. Pinton, F. Chillà, and N. Mordant, ''Intermittency in the closed flow between coaxial corotating disks,'' Eur. J. Mech. B/Fluids **17**, 535 (1998).

[54] R. H. Kraichnan, ''Anomalous scaling of a randomly advected passive scalar,'' Phys. Rev. Lett. **72**, 1016 (1994).